Chapter 2

SUMO-2 Orchestrates Chromatin Modifiers in Response to DNA Damage

Ivo A. Hendriks[1], Louise W. Treffers[1], Matty Verlaan - de Vries[1], Jesper V. Olsen[2] and Alfred C.O. Vertegaal[1]

[1]Department of Molecular Cell Biology, Leiden University Medical Center, Albinusdreef 2, 2333 ZA, Leiden, the Netherlands
[2]Novo Nordisk Foundation Center for Protein Research, Faculty of Health and Medical Sciences, University of Copenhagen, Blegdamsvej 3B, 2200 Copenhagen, Denmark.

Chapter 2 has been submitted for publication

2

ABSTRACT

Small Ubiquitin-like Modifiers play critical roles in the DNA Damage Response. To increase our understanding of SUMOylation in the DDR, we have employed a quantitative proteomics approach to identify dynamically regulated SUMO-2 conjugates upon treatment with the DNA damaging agent MMS. We have uncovered a set of 42 SUMO-2 conjugates that were upregulated in response to MMS and 35 that were downregulated, indicating a balanced role for SUMOylation in the DDR. Identified SUMO target proteins consist of interaction networks of chromatin modifiers, transcription factors, DNA repair factors and nuclear body components. SUMO-2 orchestrated chromatin modifiers include Jarid1B, Jarid1C, p300, CBP, SetDB1 and MBD1. Whereas SUMOylated Jarid1B was ubiquitylated by the SUMO-targeted ubiquitin ligase RNF4 and degraded by the proteasome in response to DNA damage, Jarid1C was SUMOylated and recruited to the chromatin to demethylate histone H3K4. Taken together, SUMO orchestrates a network of chromatin modifiers to regulate transcription in response to DNA damage.

INTRODUCTION

Posttranslational modifications (PTMs) significantly increase the functional repertoire of proteomes. PTMs range from small chemical modifications such as phosphorylation, acetylation and methylation, to small modifiers such as ubiquitin and ubiquitin-like family members (Ubls). Ubls are covalently attached to lysines in target proteins through an isopeptide bond, and thereby regulate the functions of these proteins. Moreover, modification by Ubls is a reversible process and therefore provides cells with a mechanism to facilitate a rapid response to dynamic conditions. Conjugation and removal of Ubls is coordinated by a subset of specialized and often context-specific enzymes.

Small ubiquitin-like modifiers (SUMOs) are members of the Ubl family, and have been implicated in orchestration of biological processes ranging from control of cell cycle progression and transcriptional regulation to chromatin remodeling and DNA repair [1-4]. Compared to ubiquitin, the machinery responsible for SUMO conjugation and removal consists of a relatively small subset of enzymes, even though SUMOs modify in the range of a thousand proteins in mammalian cells [5]. Furthermore, whereas ubiquitin functions in all cellular compartments, SUMOs are predominantly located in the nucleus and enriched in Promyelocytic Leukemia (PML) nuclear bodies, playing a pivotal role in the regulation of this critical subcellular domain. SUMOs display some specificity in conjugation, with the predominant consensus motif being [VIL]KxE, although SUMOylation on alternate or non-consensus motifs also occurs [6].

Our knowledge on the coordination of the DNA damage response by SUMOylation has significantly improved over the last decade [7]. As SUMOs are naturally abundant in the nucleus, they provide an effective cellular mechanism for regulating the function of proteins involved in the response to DNA damage. A significant number of studies have been published on SUMOylation with regard to regulating singular DNA damage response proteins [3, 7-11]. Whereas insight into the direct mechanistic effect of SUMO conjugation on a protein is highly interesting, there are cases where the effect of deregulation of SUMOylation on a singular target only causes a modest defect and does not always lead to a significant phenotype [12]. Instead, SUMOs are likely to regulate the function of many proteins simultaneously, which altogether is required for efficient functioning of the cell. Indeed, disruption of the SUMO machinery at the level of conjugating and deconjugating enzymes leads to embryonic lethality, associated with genome instability [13].

Advances in the field of mass spectrometry and bio-informatics have increasingly facilitated the system-wide study of PTMs. Large studies on modifications such as phosphorylation, acetylation and ubiquitylation have been published, with many thousands of target proteins being quantitatively investigated, and tens of thousands specific conjugation sites being mapped [14, 15]. Due to the relatively low abundance of SUMOylation and purification challenges of SUMO-conjugated

proteins, SUMOs still elude in-depth investigation. Progress has been made in large-scale analysis of SUMOylated proteins, especially through application of stable isotope labeling of amino acids in culture (SILAC), allowing SUMOylation to be quantitatively studied at the protein level [1, 16].

We have optimized a SUMO purification method combining harsh lysis with efficient and high-yield purification of FLAG-SUMO-conjugated proteins. This methodology was employed to study the role of SUMOylation in the cellular response to methyl methanesulfonate (MMS), a commonly utilized alkylating agent. Nearly one thousand SUMOylated proteins were uncovered, with nearly a hundred of these proteins being dynamically regulated in response to MMS treatment. A large portion of these proteins were found to be functionally related. We focused on the PML protein in addition to a pair of closely related histone H3K4me2/3 demethylases, JARID1B/KDM5B and JARID1C/KDM5C. We discovered these demethylases to be dynamically and differentially modified by SUMO-2 in response to MMS, and shed light on how SUMOylation plays a critical role in orchestrating the cellular response to DNA damage in mammalian cells by modifying dozens of proteins simultaneously, ultimately leading to a state of general transcriptional repression.

RESULTS

A Strategy to Purify FLAG-SUMO-2 Conjugates by Immunoprecipitation

SUMO-specific proteases (SENPs) are responsible for deconjugation of SUMOs from their target proteins. SUMO conjugates are notoriously difficult to purify from cells due to the robustness and high activity of SENPs upon cell lysis. To date, there are no effective and cell-permeable SENP-specific inhibitors. Thus, lysis of cells in standard buffers makes isolation of SUMO-conjugates difficult as SENPs are stable under a wide range of conditions, and act very swiftly and promiscuously to remove SUMOs from all target proteins. In order to counteract removal of SUMOs from target proteins upon cell lysis, highly denaturing conditions such as ionic detergents (SDS) or a high concentration of chaotropic agents (guanidine, urea) have to be used to inactivate SUMO-specific proteases. Facilitating efficient immunoprecipitation of SUMOylated proteins from a highly denaturing lysate is difficult as the antibodies used in such assays will likewise be denatured in these harsh buffer conditions.

In order to study SUMOylated proteins, a common approach is usage of an epitope-tagged exogenous SUMO in order to facilitate purification after lysis under highly denaturing conditions. We devised a methodology that combined harsh lysis in high concentration SDS with a one-to-one dilution step using a mild buffer that contained a high concentration of bovine serum albumin (BSA) in order to quench free SDS. For our approach, we utilized FLAG-tagged SUMO-2 stably expressed at near-endogenous levels in HeLa cells (**Figure 1A**). Investigation of the FLAG-SUMO-2 cell line by confocal fluorescent microscopy revealed a proper nuclear localization of FLAG-SUMO-2, as well as characteristic nuclear bodies scattered around the nucleus

(**Figure 1B**). SUMO-2, which is virtually identical to SUMO-3 [17], was chosen in the context of our experiment because it is the most dynamic and abundant SUMO family member [18].

Our approach facilitated denaturing lysis with accompanying inactivation of SUMO-specific proteases, and allowed highly efficient immunoprecipitation by anti-FLAG antibodies, while keeping the lysate volume relatively small to allow a high degree of enrichment. Furthermore, cells did not have to be pre-treated with (SUMO) protease inhibitors while still in culture, and likewise no addition of (SUMO) protease inhibitors was required while harvesting the cells prior to lysis.

SUMOylation Dynamics in Response to the DNA Damaging Agent MMS

SUMOylation plays a key role in the DNA Damage Response (DDR) [7], e.g., it was shown that the SUMOylation system is required for cellular responses to MMS [9, 19]. Despite the identification of a significant number of DDR components as SUMO target proteins, global insight in SUMOylation dynamics in response to DNA damage is limited. In order to quantitatively detect changes in SUMOylation of proteins during the DDR, we utilized a SILAC approach to apply differential metabolic labeling to FLAG-SUMO-2 cell lines as well as the parental HeLa cell line (**Figure 1C**). Subsequently, we treated the FLAG-SUMO-2 cells with MMS, and left another pool of FLAG-SUMO-2 cells and the parental HeLa cells untreated, prior to lysis and subsequent immunoprecipitation of FLAG-SUMO-2 (**Figure 1D**). The parental HeLa line served as an internal control to separate SUMO-2 target proteins from potential background binders. Upon treatment with MMS, SUMO nuclear bodies rapidly dispersed, indicating a role for the dissociation of these SUMO-enriched nuclear bodies in response to DNA damage (**Figure 1B**).

LC-MS Identification of Dynamically Regulated SUMOylated Proteins in Response to DNA Damage

Tryptic digests of SDS-PAGE-size-fractionated proteins were analyzed by nano-scale reversed phase liquid chromatography combined with high-resolution mass spectrometry. We performed the experiment in biological duplicate with swapped SILAC labels in order to increase confidence of discovery and to filter out contaminants, and subsequently SUMOylated proteins were identified and quantified.

We identified over 1,400 putative SUMOylated proteins, of which 800 high confidence, and 360 very high confidence. We identified 42 proteins with upregulated SUMOylation and 35 proteins with downregulated SUMOylation in response to MMS treatment (**Figure 2A**). Additionally, these 77 proteins were enriched in SUMOylation state over the parental HeLa control (**Figure 2B**). Normalization was performed around total SUMO-2/3 levels, to compensate for a slight drop of total SUMOylation proteins in response to MMS treatment. Interestingly, while a modest decrease in the total SUMOylated pool of proteins was observed, various SUMOylated proteins were upregulated, including p300, CBP, PARP-1 and JARID1C

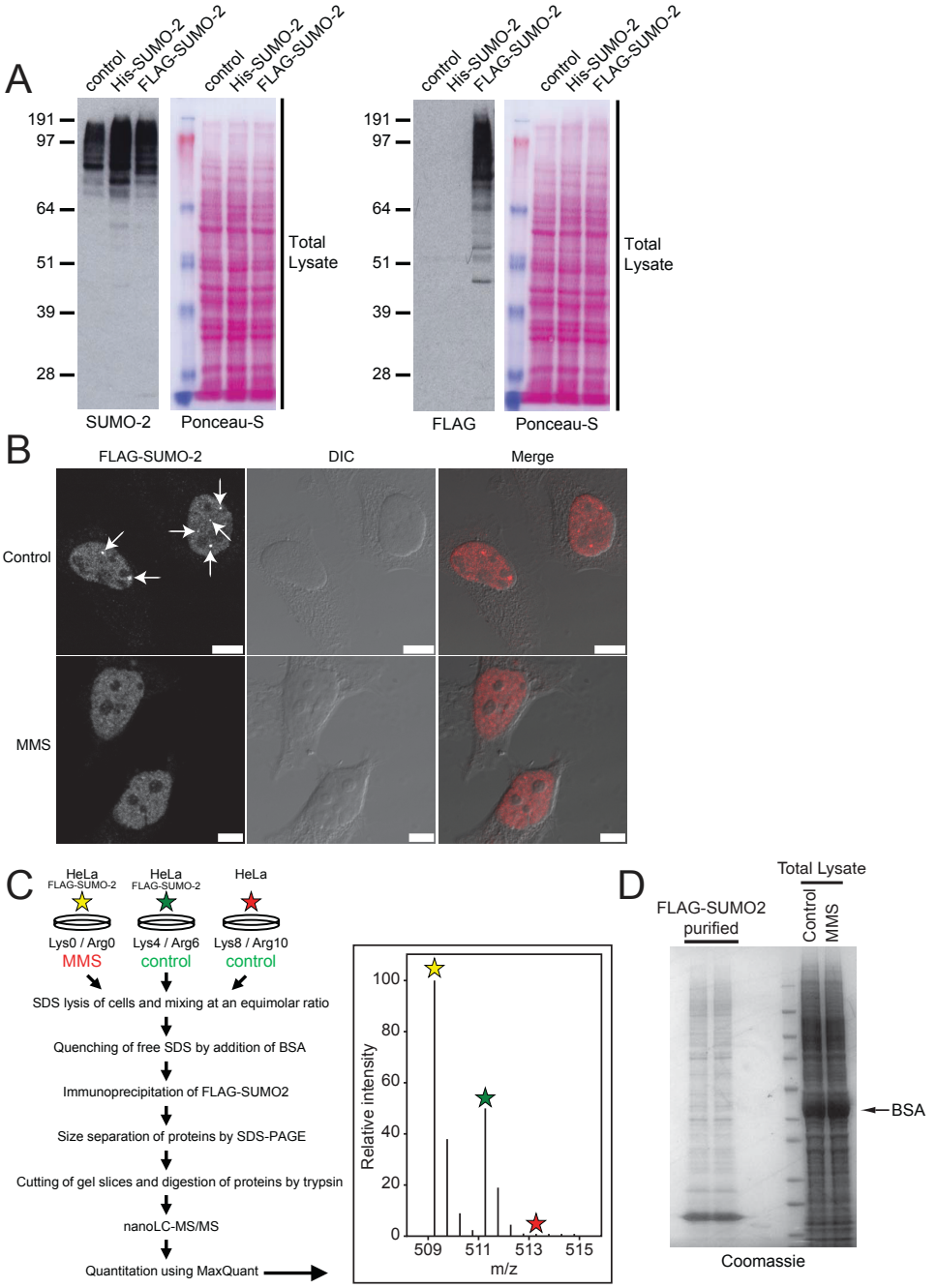

Figure 1. Generation of cell lines stably expressing FLAG-tagged SUMO-2, and purification of FLAG-SUMO-2 conjugates following MMS treatment.

A) HeLa cells were infected with a bicistronic lentivirus encoding FLAG-SUMO-2 and GFP separated by an Internal Ribosome Entry Site (IRES). Cells stably expressing low levels of FLAG-SUMO-2 were selected by flow cytometry. Total lysates were analyzed by immunoblotting to confirm the expression of FLAG-SUMO-2. Ponceau-S staining is shown as a loading control.

(**Figure 2C**). Scatter plot analysis of SUMOylation state in response to MMS versus SUMOylation enrichment over parental cells revealed that targets responded more extremely to MMS if they were highly SUMOylated, and these highly SUMOylated proteins showed a tendency to be downregulated in response to MMS (**Figure 2B**). One of the most striking changes we observed was the downregulation of SUMOylated demethylase JARID1B, whereas SUMOylation of the closely related family member JARID1C was upregulated in response to MMS.

Characterization of a SUMO-regulated System-wide Response to DNA Damage

Gene Ontology analysis of SUMO-regulated proteins provided more insight into the dynamic regulation of the DNA damage response by SUMO (**Figure 2D**). Proteins with increased SUMOylation showed enrichment in categories such as signal transduction in response to DNA damage, DNA metabolism, and positive regulation of transcription. Conversely, proteins with decreased SUMOylation were found to be involved in negative regulation of transcription, negative regulation of gene expression, and a wide range of chromatin modifications and organization. Upregulated SUMO targets were moderately enriched for nuclear localization and localization in non-membrane organelles, whereas downregulated SUMO targets were heavily enriched for localization in nuclear bodies, in chromatin, and otherwise in the nucleus. This finding was in agreement with the observed dissociation of SUMO-enriched nuclear bodies upon MMS treatment by confocal fluorescent microscopy (**Figure 1B**).

STRING network analysis of all SUMO-regulated proteins in response to MMS identified half of these proteins to be known or predicted interactors to each other (**Figure 2E**), giving strong backing to the theory of dynamic regulation by SUMO of groups of functionally related proteins [20, 21]. Of special note is the p300/CBP/PML main cluster, which functionally connects a quarter of all identified SUMO-regulated proteins to each other. This cluster is nearly equally composed of up- and down-regulated SUMOylated proteins, displaying SUMO's ability to modulate proteins in a balanced manner.

B) Stable cell lines were investigated by Z-stacked confocal fluorescent microscopy to confirm nuclear localization of FLAG-SUMO-2. Characteristic SUMO nuclear bodies are indicated with arrows. Upon MMS treatment (0.02% for 90 minutes), SUMO nuclear bodies dispersed. Scale bars represent 5 µm.
C) Schematic representation of the SILAC proteomics workflow. One set of parental HeLa cells and two sets of HeLa cells expressing FLAG-SUMO-2 were differentially SILAC labeled (K0R0/K4R6/K8R10). One labeled FLAG-SUMO-2 set was treated with 0.02% MMS for 90 minutes. The entire experiment was repeated with reversal of SILAC labels. Subsequent to treatment, cells were lysed and lysates were mixed in an equimolar ratio before enriching SUMOylated proteins by FLAG-immunoprecipitation. Enriched fractions were size-separated by SDS-PAGE, digested by trypsin, analyzed using LC-MS/MS, and quantified and analyzed using the software packages MaxQuant and Perseus.
D) Coomassie analysis of total lysate sample versus FLAG-purified SUMOylated proteins, prior to in-gel digestion and analysis by mass spectrometry.

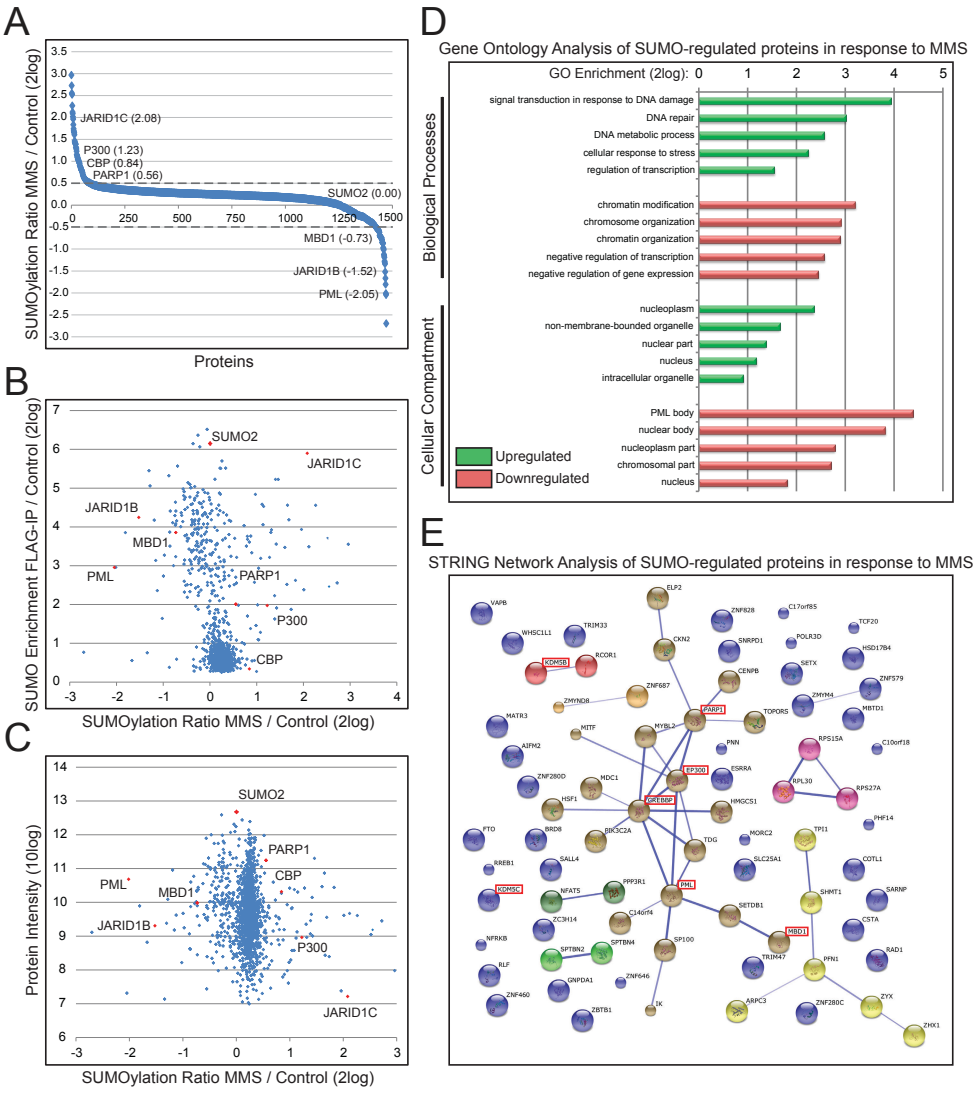

Figure 2. Analysis of the mass spectrometry data reveals highly enriched interaction clusters.
A) Overview of identified protein numbers versus their 2-log SUMOylation SILAC ratio in response to MMS. 42 targets were SUMO-upregulated (>0.5), and 35 targets were SUMO-downregulated (<-0.5). Selected proteins of interest and SUMO-2 are indicated with their respective 2-log ratio.
B) Scatter plot analysis of 2-log SUMOylation SILAC ratios in response to MMS, versus 2-log SUMOylation SILAC ratio enrichment over the parental control. Selected proteins of interest and SUMO-2 are indicated.
C) Scatter plot analysis of 2-log SUMOylation SILAC ratio in response to MMS, versus 10-log quantified protein intensity. Selected proteins of interest and SUMO-2 are indicated.
D) Summary of Gene Ontology (GO) analysis of identified up- and down-regulated SUMOylated proteins in response to MMS. Relative GO enrichment of regulated SUMOylated proteins versus the human proteome is indicated for the Biological Process (BP) and Cellular Compartment (CC) categories.

Differential SUMOylation of Chromatin Modifiers in Response to MMS

On further investigation of selected target proteins by immunoblotting, we confirmed the differential SUMO-regulation of these proteins, as initially identified by mass spectrometry (**Figure 3A**). P300 and CBP, two important transcriptional co-activators, were found to be more highly SUMOylated in response to MMS. A higher SUMOylation of these proteins is indicative of reduced function, which would lead to overall transcriptional repression [22]. We verified the increase in Poly ADP-Ribose Polymerase 1 (PARP-1) SUMOylation (**Figure 3A**), and also confirmed the slight decrease in total SUMOylated proteins after MMS treatment by immunoblot (**Figure 3B**).

Strikingly, we identified the histone 3 lysine 4 di- and tri-methylation specific demethylases JARID1B and JARID1C as being differentially regulated by SUMO in response to MMS (**Figure 3A**). Whereas JARID1C SUMOylation was increased after MMS treatment, JARID1B SUMOylation was no longer detectable. Furthermore, upon confirmation that the upper band on the immunoblot corresponded to full-length endogenous JARID1B by shRNA-mediated knockdown of the protein in HeLa and U2OS cells (**Figure S2**), we discovered that the JARID1B protein was swiftly degraded in its entirety during MMS treatment.

The SUMOylated form of Promyelocytic Leukemia (PML) protein, a tumor suppressor protein, has a key function in structuring nuclear bodies [23-25]. We confirmed the rapid loss of SUMOylation after MMS treatment by immunoblot, and the dissociation of PML nuclear bodies by confocal fluorescent microscopy (**Figure 3C**). We also verified the decreased SUMOylation of Methyl-CpG-binding domain protein 1 (MBD1) after MMS treatment by immunoblot (**Figure 3A**).

SUMOylated JARID1B and PML are Degraded by the Ubiquitin-Proteasome in Response to MMS

We investigated the involvement of the ubiquitin-proteasome by combining MMS treatment of cells with the proteasome inhibitor MG-132. For this purpose, we used a U2OS cell line stably expressing His-SUMO-2 at low levels, to accommodate nickel-ion affinity chromatography to enrich and investigate SUMOylated proteins. When treating cells with MMS in a time course experiment, we found SUMOylated JARID1B and PML to be rapidly degraded, as observed earlier in HeLa cells (**Figure 4**). Similarly, we found JARID1B to be degraded in its entirety within two hours of MMS treatment. When pre-treating cells with MG-132 before addition of MMS, the

E) STRING network analysis of all regulated SUMOylated proteins in response to MMS. Proteins with interactions are connected by a blue line and colored similarly, and separate clusters are colored differently. Thickness of the blue line connecting proteins is representative of confidence in the interaction. 39 out of 77 identified SUMO-regulated proteins (51%) are part of an interaction cluster. There are 38 observed interactions versus 5 randomly expected interactions ($p < 1*10-10$). Selected proteins of interest are highlighted in red. An expanded STRING analysis with additional predicted interactor nodes is available (Figure S1A), as well as an analysis with SUMO2 added to the network (Figure S1B).

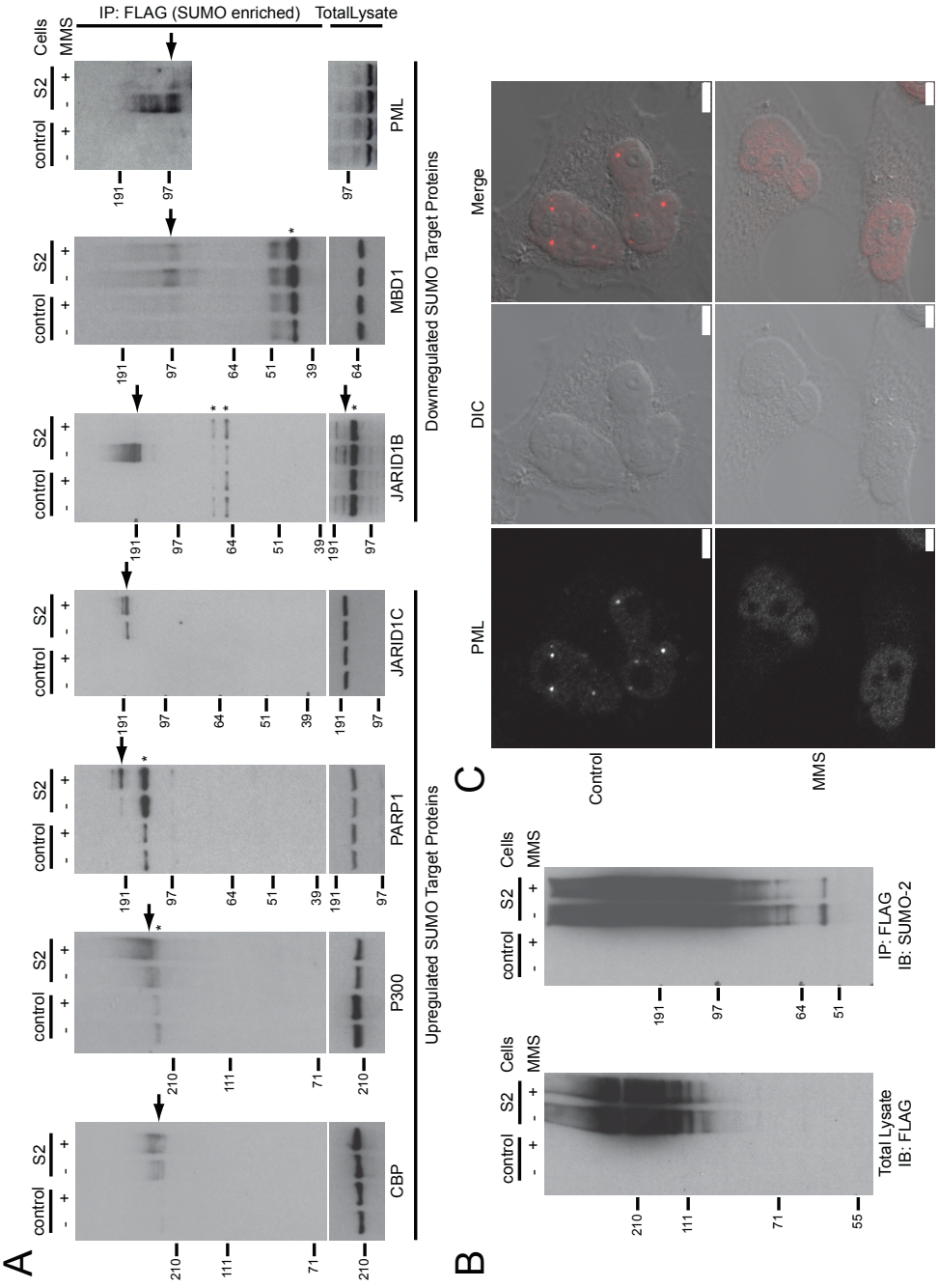

Figure 3. Confirmation of mass spectrometry results.

A) HeLa cells and HeLa cells stably expressing FLAG-SUMO-2 were either mock treated or treated with MMS. Cells were lysed, and FLAG-IP was performed to enrich SUMOylated proteins. Total lysates and SUMO-enriched fractions were analyzed by immunoblotting to confirm the SUMO regulation of the indicated proteins.

degradation of JARID1B protein was blocked entirely. Furthermore, the degradation of SUMOylated JARID1B and PML was prevented, and accordingly there was a modest increase of SUMOylated proteins with increasing length of MMS treatment in the presence of MG-132.

Degradation of SUMOylated JARID1B and PML is Controlled by the SUMO-specific Ubiquitin E3 Ligase RNF4

RNF4 is a SUMO-specific ubiquitin E3 ligase that recognizes poly-SUMOylated target proteins through its SUMO Interaction Motifs (SIMs), and subsequently facilitates the ubiquitylation and degradation of these proteins [26]. We investigated the involvement of RNF4 by repeating the experiment essentially as described above, but using shRNA-mediated depletion of endogenous RNF4 prior to MMS treatment instead of using MG-132 to block the proteasome (**Figure 5A**). We observed an accumulation of highly SUMOylated PML when depleting endogenous RNF4 prior to treatment with MMS. When treating cells with arsenic trioxide as a control [27], PML was found to be more heavily poly-SUMOylated, and additional depletion of endogenous RNF4 resulted in a further increase of highly SUMOylated forms of PML. Similarly, SUMOylated JARID1B was retained after MMS treatment when endogenous RNF4 was depleted. In contrast to PML, we observed no notable change in JARID1B's SUMOylation state in response to arsenic treatment.

Simultaneously, we investigated JARID1C, and confirmed the increase in SUMOylation of this protein in response to MMS (**Figure 5A**). Depletion of RNF4 did not further increase JARID1C SUMOylation in response to MMS, and similar to JARID1B, SUMOylation of JARID1C was not altered in response to arsenic treatment. Interestingly, when observing the total pool of SUMOylated proteins, we noted a considerable increase of these proteins when endogenous RNF4 was depleted. It is plausible to assume that RNF4 regulates many poly-SUMOylated proteins, and that its absence would result in an accumulation of its SUMOylated targets. Still, as indicated with the differential effect of RNF4 depletion on PML, JARID1B and JARID1C, it appears that the accumulation of SUMOylated proteins was restricted to RNF4 target proteins.

Dissociation of PML Nuclear Bodies in Response to MMS Treatment is Modulated by SUMO-specific Ubiquitin E3 Ligase RNF4

Dissociation of PML bodies in response to DNA damage has been reported before [28], and is thought to mediate redistribution of proteins from these nuclear depots to sites of DNA damage [29]. We observed that depletion of RNF4 prevents poly-SUMOylated PML from being ubiquitylated and degraded (**Figure 5A**).

B) Immunoblotting verification of overall level of SUMO-conjugated proteins in the total lysates and SUMO-enriched fractions after MMS treatment and FLAG-IP.
C) Cell lines stably expressing FLAG-SUMO-2 were investigated by confocal fluorescent microscopy for the presence of PML nuclear bodies. Upon MMS treatment, PML bodies rapidly dispersed. Scale bars represent 5 μm.

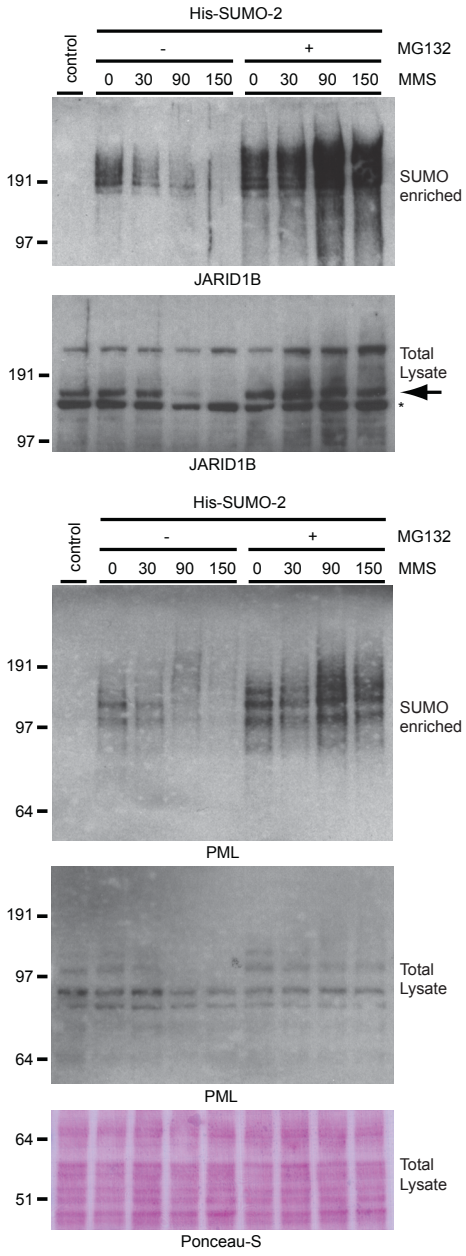

Similarly, we investigated the dissociation of PML bodies in response to MMS using Z-stacked confocal microscopy, in a control setting and with depletion of endogenous RNF4 by shRNA-mediated knockdown (**Figure 5B**). In addition to the fields of cells shown in the example figure, we selected multiple fields in an unbiased fashion and counted cells and their respective PML bodies until we quantified at least 200 cells per experimental condition (**Figure 5C**). In the control, we observed that within 45 minutes of treatment with MMS, most PML-bodies had disassembled, and after 90 minutes virtually no PML bodies could be detected. When RNF4 was depleted in cells prior to MMS treatment, the large majority of cells still retained their PML bodies after 45 minutes of MMS treatment, and even after 90 minutes over a quarter of all cells retained a significant amount of PML bodies. These findings show that PML bodies dissociate through RNF4-mediated ubiquitylation and subsequent degradation of SUMOylated PML in response to MMS.

Cells enter a transcriptionally-repressed state in response to MMS treatment

As JARID1B and JARID1C are H3K4me2/3-specific demethylases, we investigated the effect of MMS on the global level of the transcriptional activity markers H3K4me2 and –me3 in U2OS cells (**Figure 6A**). We observed that with

Figure 4. SUMOylated JARID1B and PML are rapidly degraded by the proteasome upon MMS treatment.

U2OS cells stably expressing His-tagged SUMO-2 were treated with 0.02% MMS for the indicated amount of time. One set of cells was additionally treated with the proteasome inhibitor MG-132 at 10 μM. Cells were lysed, and His-pulldown was performed to enrich SUMOylated proteins. Total lysates and SUMO-enriched fractions were analyzed by immunoblotting using antibodies against JARID1B and PML. Ponceau-S staining was performed on total lysate fractions as a loading control.

increasing amounts of DNA damage induced by treating cells with increasing dosage of MMS, the global H3K4me2 and H3K4me3 levels drop in a dynamic fashion in concurrence with the amount of DNA damage, indicating that the differential regulation of JARID1B and JARID1C by SUMOylation resulted in increased demethylase activity.

In these experiments, we also verified the levels of the transcriptional repressive marks H3K9me2 and –me3, since our screen also indicated the dynamic regulation by SUMOylation of the H3K9 methylases SETDB1 and MBD1 (**Figure 3A**). Interestingly, global levels of H3K9me2 and H3K9me3 were elevated as more DNA damage is incurred. Overall, our results show that SUMOylation orchestrates multiple histone demethylases and methylases in response to DNA damage, resulting in a state of transcriptional inhibition, as cells are likely to decrease transcriptional activity to prioritize DNA repair processes [30].

H3K4me2/3-specific demethylase JARID1C is recruited to the chromatin in response to DNA damage

Investigation of JARID1C total protein levels after MMS treatment revealed no substantial decrease, as opposed to JARID1B. In order to explain the decreased levels of H3K4me2/3, we studied the subcellular localization of these JARID1 family members in U2OS cells upon MMS treatment using a biochemical approach by separating the cells into cytoplasmic, soluble nucleoplasmic and chromatin-associated fractions (**Figure 6B**). As anticipated, we found JARID1B to be located exclusively in the chromatin-associated fraction prior to DNA damage, with JARID1B levels in the soluble nucleoplasmic fraction being undetectably low. Furthermore, MMS treatment resulted in a swift chromatin-associated loss of JARID1B as expected from the global drop in JARID1B. Similar results were acquired in HeLa cells (**Figure S3B**). Consistently, we found the known JARID1B targets *JUN* and *MCL1* to be upregulated in response to MMS treatment by quantitative PCR (**Figure S3A**).

Remarkably, we found JARID1C to be localized mainly in the soluble nucleoplasmic fraction, and not in the chromatin-associated fraction prior to DNA damage (**Figure 6B**). It is therefore plausible to assume that JARID1C exists in a mostly inactive form in cells under normal conditions, whereas JARID1B is chromatin-associated and likely continuously modulates the H3K4me2/3 state of its specific target regions. Strikingly, upon MMS treatment of cells we found that JARID1C is relocated from the nucleoplasmic fraction to the chromatin-associated fraction, indicating a novel activation of this H3K4me2/3 demethylase in response to DNA damage (**Figure 6B**). Furthermore, while we observed the degradation of JARID1B, the total level of JARID1C remained unchanged, indicative of a relocation of virtually the entire protein pool of JARID1C from the soluble nucleoplasmic fraction to the chromatin. Similar results were obtained in HeLa cells (**Figure S3B**).

We investigated the SUMOylation state of JARID1C in the chromatin-associated fraction by performing the cellular fractionation assay in U2OS stably expressing

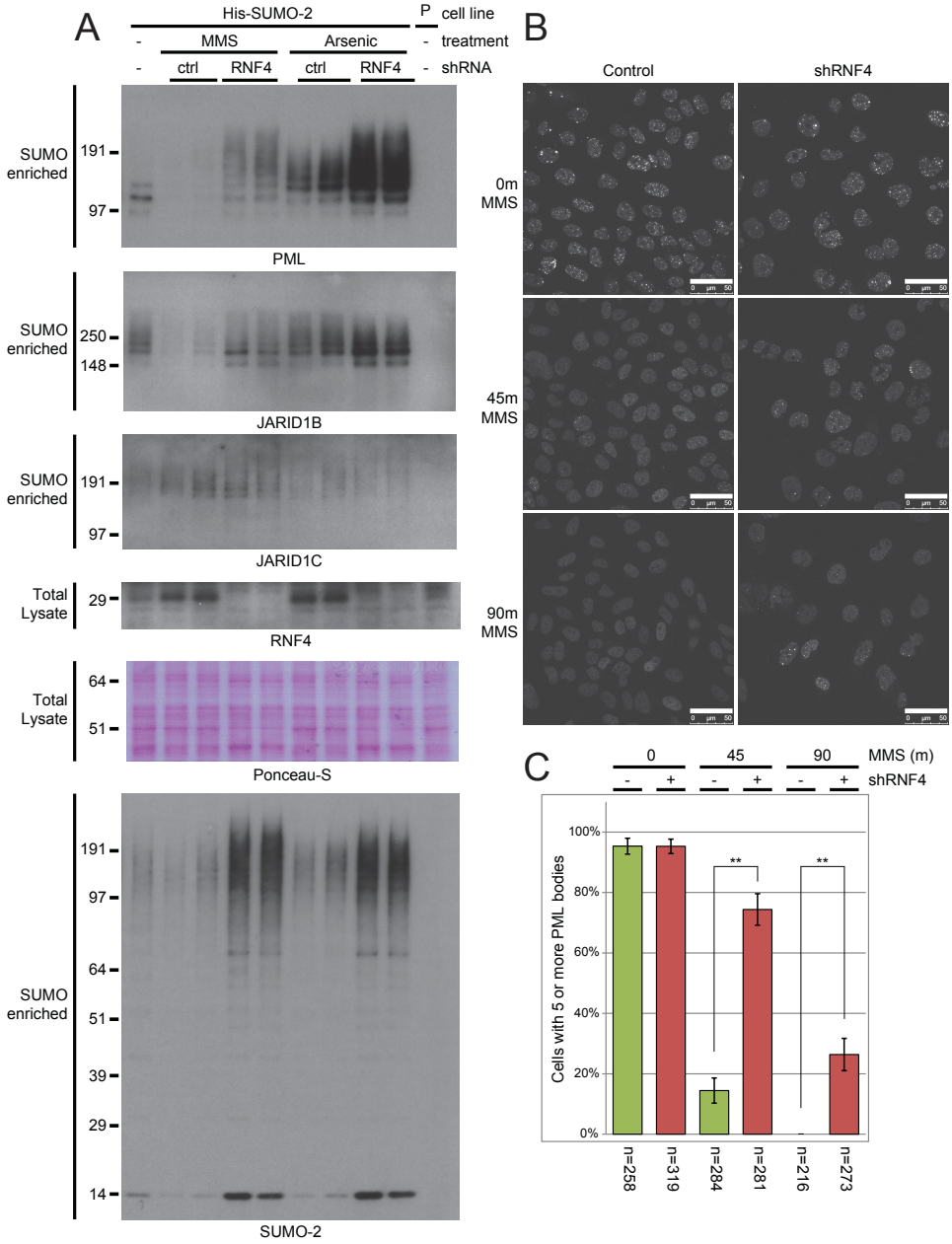

Figure 5. Degradation of SUMOylated JARID1B and PML is mediated by the SUMO-targeted ubiquitin ligase RNF4.

A) U2OS cells stably expressing His-tagged SUMO-2 were treated with 0.02% MMS or 1 µM arsenic trioxode for 90 minutes or 4 hours, respectively. One set of cells was additionally depleted for RNF4 by infection with a lentiviral knockdown construct. After treatment, cells were lysed, and His-pull-down was performed to enrich SUMOylated proteins. SUMO-enriched fractions were analyzed by immunoblotting using antibodies against PML, JARID1B, JARID1C and SUMO. Total lysate fractions were analyzed by immunoblotting for depletion of RNF4, and analyzed by Ponceau-S as a loading

His-SUMO-2, and then enriching SUMO-2 by nickel-ion affinity chromatography. Here, we found that there is a small amount of SUMOylated JARID1C present at the chromatin before MMS treatment (**Figure S3C**). Upon MMS treatment, the amount of SUMOylated JARID1C in the chromatin-associated fraction increased considerably, in line with the earlier observed increase in JARID1C SUMOylation in the total protein pool. Similar results were found in HeLa cells stably expressing His-SUMO-2 (**Figure S3C**). Our findings implicate that the SUMOylation of JARID1C plays a role in its location at the chromatin.

JARID1C demethylates global H3K4me2/3 in response to DNA damage

Overexpression of a GFP-tagged JARID1C in U2OS cells allowed us to investigate the effect of its increased presence on global H3K4me3, by utilizing confocal fluorescent microscopy (**Figure 6C**). In cells overexpressing GFP-JARID1C, we observed that the protein localized exclusively to the nucleus, as anticipated. Overexpression of GFP-JARID1C by itself resulted in a slight decrease of global H3K4me3, likely as a result of a larger fraction of JARID1C reaching the chromatin and demethylating H3K4me3. However, overexpression of GFP-JARID1B at similar or lower levels as compared to GFP-JARID1C resulted in a near complete removal of H3K4me3 (**Figure S3D**), indicative of efficient localization of JARID1B to the chromatin under standard conditions. Furthermore, MMS treatment of U2OS cells resulted in a similar slight decrease of global H3K4me3, as noted before, due to changes in the chromatin remodeling landscape changing in response to MMS treatment. Strikingly, when cells overexpressing GFP-JARID1C were treated with MMS, we observed a dramatic drop of H3K4me3 (**Figure 6C**). We propose that upon treatment with MMS, GFP-JARID1C is recruited to the chromatin analogous to endogenous JARID1C, where it then actively removes H3K4me3.

Overall, our study indicates that SUMOylation orchestrates a complex network of chromatin modifiers to regulate transcriptional responses to DNA damage (**Figure 7**).

DISCUSSION

SUMO Orchestrates the Cellular Response to DNA damage

Small Ubiquitin-like Modifiers play critical roles in the DNA Damage Response [3, 7]. To increase our understanding of the roles of SUMOylation in the DDR, we

control.

B) U2OS cells were treated with MMS for the indicated amount of time. One set of cells was additionally depleted for RNF4 by infection with a lentiviral knockdown construct. Groups of cells were investigated by Z-stacked confocal fluorescence microscopy for the presence of PML bodies. Scale bars represent 50 μm.

C) Multiple fields of cells were recorded as in Figure 5B. Cells were counted, PML bodies were quantified in every cell, and scored for the presence of at least five PML bodies. The number of quantified cells is indicated below each experiment. Error bars represent 2x SEM. ** $p < 1*10^{-15}$

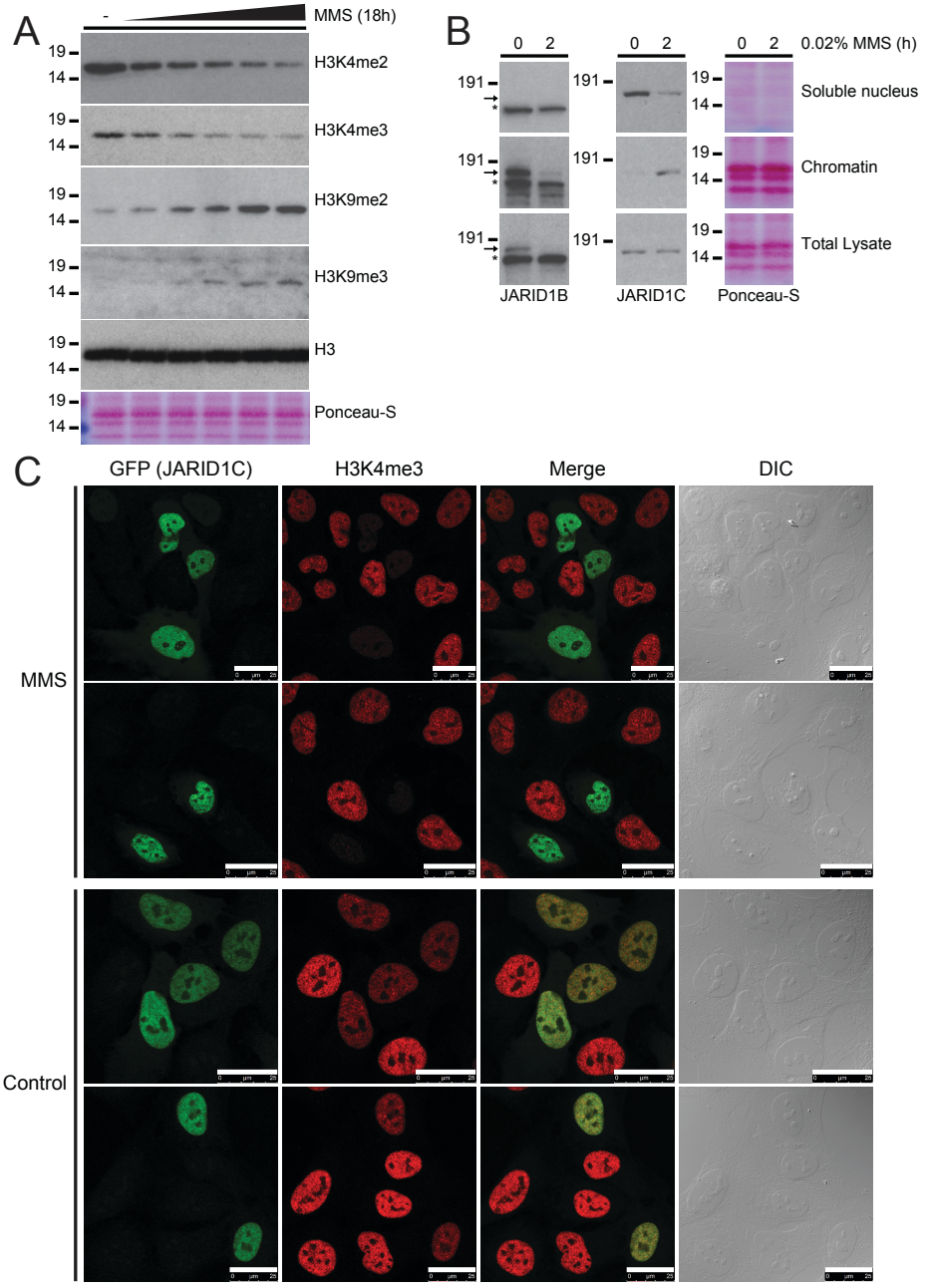

Figure 6. H3K4me2/3-specific demethylase JARID1C is recruited to the chromatin in response to DNA damage.

A) U2OS cells were treated with the indicated dose of MMS overnight. Cells were lysed and analyzed by immunoblotting for H3K4me2, H3K4me3, H3K9me2 and H3K9me3. Immunoblotting for Histone H3 and Ponceau-S are shown as loading controls.

B) U2OS cells were mock treated or treated with 0.02% MMS for 90 minutes, and subsequently cellular fractionation was performed to separate the soluble nucleoplasmic fraction from the

have performed a systematic investigation to uncover the target proteins of the human SUMO family member SUMO-2 in response to DNA damage. A quantitative proteomics approach was used to identify dynamically regulated SUMO-2 conjugates upon treatment with the DNA damaging agent MMS. Previously, it has been demonstrated that eukaryotic cells deficient for SUMOylation are sensitive to this compound [9, 19]. We have uncovered a set of 42 SUMO-2 conjugates that were upregulated in response to MMS and 35 that were downregulated, indicating that SUMOylation plays a balanced role in the DDR. Identified SUMO target proteins included interaction networks of chromatin modifiers, transcription factors, DNA repair factors and nuclear body components.

SUMO Coordinates Global Transcriptional Repression in Response to DNA Damage

Cells respond to DNA damaging agents by globally altering their transcriptional programs [31]. Transcriptome-wide studies have indicated that around 30% of mRNAs are altered in response to MMS treatment [32]. This response includes the downregulation of genes involved in protein synthesis to enable cells to focus on nucleic acid metabolism. Moreover, genes involved in the DDR are upregulated in response to MMS [33]. Mechanisms behind transcriptional reprogramming are less clear, but the regulation of RNA polymerase II in response DNA damage is a key focus of the field [30].

Our results indicate that SUMO plays an important role in the orchestration of global transcriptional reprogramming in response to MMS at the chromatin level. Firstly, trimethylation of histone H3K4 is a key chromatin mark of active genes [34] associated with SUMOylation [35] and was found to be decreased upon MMS treatment. Mechanistically, this could be explained by recruitment of Jarid1C to the chromatin upon MMS treatment, related to its SUMOylation. We have also provided evidence that Jarid1C and MMS cooperate to reduce global H3K4Me3. Combined, these findings indicate a novel role for Jarid1C in the DNA damage response to decrease H3K4me3.

Secondly, global levels of the transcriptional repressive marks H3K9me2/3 [34], were found to be increased upon MMS treatment. Mechanistically, this could be explained by reduced SUMOylation of Methyl-CpG-Binding domain 1 (MBD1) in response to MMS. MBD1 forms a repressive complex with the methylase SETDB1 to facilitate methylation of H3K9, and SUMOylation of MBD1 has been reported

chromatin. Soluble nucleoplasmic fractions, chromatin fractions, and total lysates were analyzed by immunoblotting for JARID1B and JARID1C. Ponceau-S staining of the histones is shown as a loading and fractionation control.

C) U2OS cells were transfected with GFP-JARID1C, and either mock treated or treated with 0.02% MMS for 90 minutes. Subsequently, cells were fixed and investigated by confocal fluorescent microscopy to check for the presence of JARID1C (GFP) and the level of H3K4me3. The presence of GFP-JARID1C or MMS treatment resulted in a minor drop in global H3K4me3, whereas the combination of both GFP-JARID1C and MMS resulted in an intense drop of global H3K4me3. Scale bars represent 25 µm.

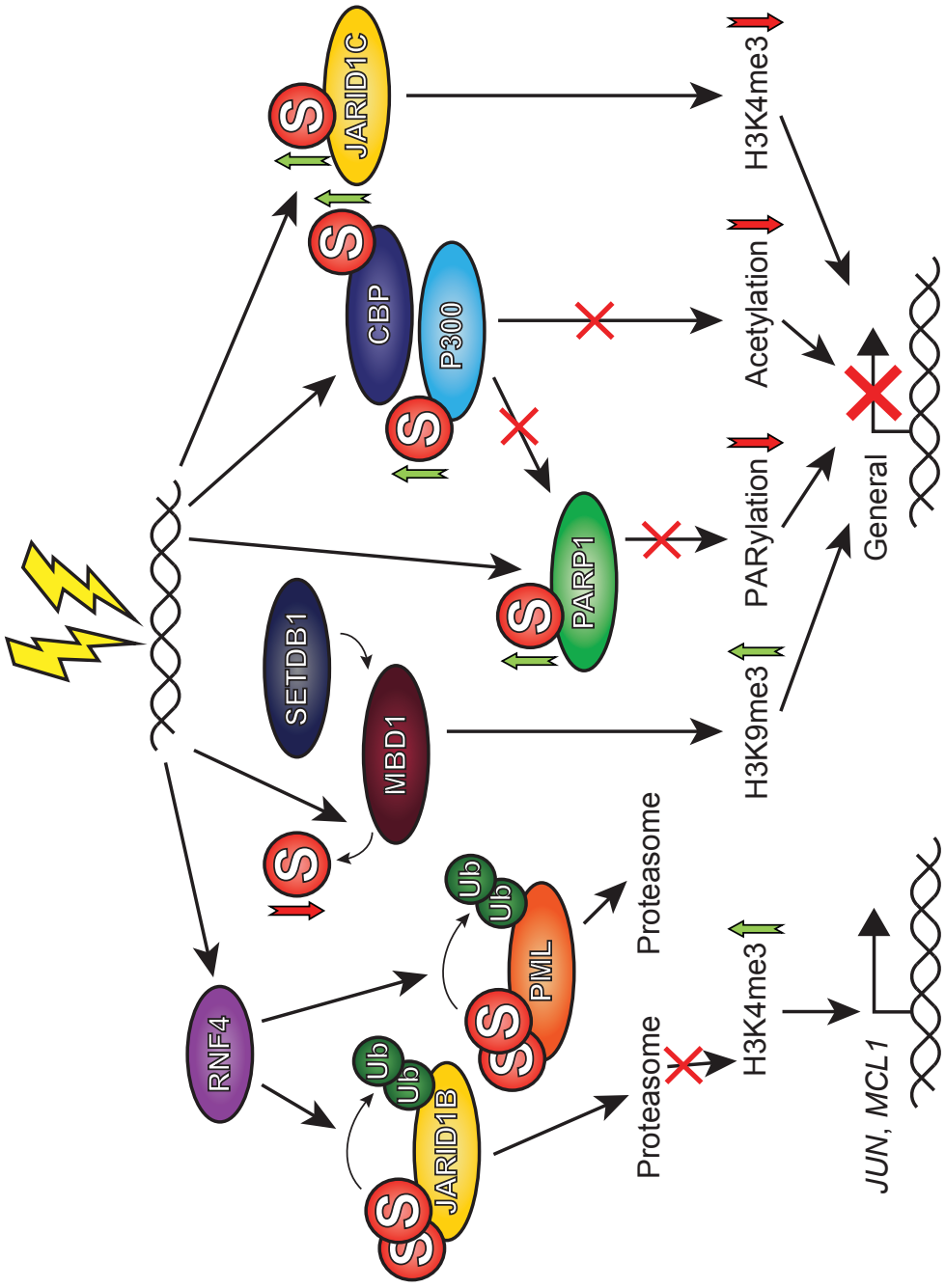

Figure 7. SUMOylation mediates the cellular response to alkylating DNA damage at the chromatin remodeling and transcriptional regulation level.
Schematic overview of the effect of SUMOylation on various key proteins involved in the cellular response to DNA damage, and the downstream effect on chromatin remodeling and transcriptional regulation.

to counteract its interaction with SETDB1 and thus prevent its repressive function [36]. The decrease in MBD1 SUMOylation that we observed in our study is therefore expected to increase the interaction with SETDB1, concomitantly increasing the methylation of H3K9. We also discovered an increased SUMOylation of SETDB1 itself, and although SETDB1 has been reported to interact with SUMO [37], this is the first time that covalent SETDB1 SUMOylation is reported.

Thirdly, we observed increased SUMOylation of the acetyl transferases CBP and p300. These acetyl transferases acetylate all four core histones, which is expected to cause nucleosome instability [38]. Both acetyl transferases contain a repressive domain including two consensus motifs for SUMOylation. SUMOylation of CPB and p300 was previously shown to decrease the activity of these proteins [22]. Here, we showed that the SUMOylation of both proteins was increased in response to DNA damage, which would consequently lead to reduced histone acetylation and therefore reduced transcriptional activity.

Combined, orchestration of these chromatin modifiers by SUMOylation contributes to a transcriptional repressive environment by decreasing H3K4me2/3, increasing H3K9me2/3 and decreasing histone acetylation. Although transcriptional inhibition was the dominant effect orchestrated by SUMOylation, it was not an exclusive phenomenon as *JUN* and *MCL1* were upregulated (**Figure S3A**). Mechanistically, this could be explained by the degradation of JARID1B since JARID1B actively controls a set of cell cycle and DNA damage response proteins [39]. JARID1B and 1C deregulation has been associated with various types of cancer [40-43].

SUMO Group Modification in Response to DNA Damage

STRING analysis revealed that half of the identified SUMO-2 target proteins that were responsive to DNA damage are known to functionally interact. A quarter of all identified proteins even reside in one single interaction cluster. This most striking cluster we identified contains many functionally relevant proteins such as PML, SP100, TDG, CBP, P300, PARP1, TOPORS, MDC1, HSF1, MITF, SETDB1 and MBD1, among others, only highlighting a subsection from this cluster. A further addition of 10% highest-scoring predicted interactor nodes connects half of all identified dynamically SUMOylated proteins in one single interaction cluster (**Figure S1A**). Coordination of these protein networks by SUMOylation is an efficient manner for rapid regulation of functional protein groups via post-translational modification. Group modification by SUMO in response to MMS in yeast was described previously [20, 21], but differs from our findings as in yeast the DNA damage response was centered around homologous recombination whereas in human cells we observed a response tailored towards DNA repair, transcriptional regulation and chromatin remodeling.

Crosstalk between SUMOylation and other PTMs in Response to MMS Treatment

SUMOylation of CBP and P300 was increased in response to MMS, which implied

reduced ability to acetylate their target proteins [22]. Interestingly, in addition to histones, one of these target proteins is Poly [ADP-ribose] Polymerase 1 (PARP1), which requires its acetylated state in order to PARylate its targets [44], including histone H3 [45], thus functioning as a transcriptional co-activator by organizing a permissive chromatin environment. Correspondingly, we identified PARP1 itself to be increasingly SUMOylated after MMS treatment, which has been implied to further inhibit its acetylation by P300 [44], in turn leading to an additional diminishment of PARP1's activity. The decrease of PARP1 activity would then lead to loss of histone H3 PARylation, in turn paving the way for the JARID1 family members to demethylate H3K4me3 [46], leading to inhibition of transcription. Interestingly, the ubiquitin and SUMO E3 ligase TOPORS has been reported to reside in PML bodies and to mediate PARP1 SUMOylation [47, 48]. As PML bodies dissociate after MMS treatment, TOPORS may then be free to SUMOylate PARP1. These findings implicate that SUMOylation, acetylation, PARylation and demethylation are orchestrated in response to DNA damage and shed light on how different post-translational modifications can cooperate to mediate transcriptional inhibition.

SUMO-Targeted Ubiquitin Ligases in the DNA Damage Response

We have shown here that proteasomal degradation of SUMOylated JARID1B and SUMOylated PML in response to DNA damage is mediated by the SUMO-targeted ubiquitin ligase RNF4. Interestingly, initial studies already pointed to a role for RNF4 in transcriptional regulation [49, 50]. In response to DNA damage, increased target SUMOylation and activation of RNF4 can also allow for recruitment of a specific subset of repair proteins [51, 52]. Previously, the Mediator of DNA-damage checkpoint 1 (MDC1) protein was identified as a SUMOylated target protein that is subsequently ubiquitylated by RNF4 in response to ionizing radiation [53-56]. RNF4 ubiquitylated SUMOylated MDC1 leading to its subsequent degradation by the proteasome, an event that is necessary to facilitate proper progression of homologous recombination repair. In our study, we also observed an increase of MDC1 SUMOylation in response to MMS.

Regulation of SUMOylated PML and the PML fusion protein PML-RARα by RNF4 were previously found to occur in response to arsenic trioxide [27, 57]. Overall, RNF4 is thus involved in coordinating transcriptional reprogramming, DNA repair and nuclear bodies in response to DNA damage via the ubiquitin-proteasome pathway. Furthermore, SUMO-targeted ubiquitin ligases also play other roles in the DDR since the SUMO-targeted ubiquitin ligase RNF111 exhibits nonproteolytic ubiquitylation of SUMOylated XPC, thereby facilitating the DNA damage response [58].

PML nuclear bodies

The PML protein was found as one of the SUMO-2 target proteins that is downregulated in response to MMS. PML is a key component of this nuclear substructure

and PML SUMOylation is critical for integrity of this subnuclear structure [23-25, 59], and the rapid loss of SUMOylation upon MMS treatment resulted in dissociation of these nuclear bodies, enabling release of the stored proteins into the nucleoplasmic fraction. Processes such as the DNA damage response, induction of apoptosis and induction of senescence are all linked to the dissociation of these PML bodies [29]. Degradation of SUMOylated PML leads to dissociation of nuclear bodies which in turn is thought to release repair factors such as RAD51, MRE11 and BRCA1 into the nucleus [60, 61]. We additionally discovered the PML-body component SP100 to be reduced for SUMOylation after MMS treatment, coinciding with the breakdown of the PML bodies where it normally resides. SP100 is encoded by a tumor suppressor gene and the SP100 protein recruits the transcriptional repressor HP1 to the chromatin where it specifically binds to methylated H3K9, further contributing to transcriptional repression in response to DNA damage [62, 63]. In addition to releasing SP100 from the PML bodies after MMS treatment, a reduction in SUMOylation of this protein could enhance SP100-mediated recruitment of HP1, as SUMOylation of SP100 occurs at the site where it normally binds to HP1 [64].

Summary and future perspective

In summary, we have studied the role of SUMOylation in response to DNA damage, uncovering a co-regulated group of SUMO target proteins, including a significant number of chromatin modifiers that cooperate to decrease global transcription upon DNA damage. Our study uncovers a tight link between the role of SUMOylation in the DNA damage response and the role of SUMOylation in transcriptional regulation, the two key areas of SUMOylation research. Detailed functional analysis of proteins identified in this project will further increase our insight in the role of SUMOylation in the DNA damage response. We believe therefore that the set of dynamically regulated proteins identified in our study represents a valuable resource for the scientific community. Future studies on the role of SUMOylation in the cellular responses to different types of DNA damage will undoubtedly further increase our understanding of the role of this dynamic post-translational modification with respect to genome stability.

EXPERIMENTAL PROCEDURES

Plasmids

The SUMO-2 we described and used in this manuscript has the following amino acid sequence: MSEEKPKEGVKTENDHINLKVAGQDGSVVQFKIKRHTPLSKLMKAYCERQGLSMRQIRFRFDGQPINETDTPAQLEMEDEDTIDVFQQQTGG [65]. We generated a FLAG-His6-SUMO-2 construct by introducing a Flag tag encoding oligonucleotide in the PstI site of the plasmid pLV-CMV-His6-SUMO-2 using the following primers: 5'-GATGGACTACAAGGACGACGATGACAAGCTGCA-3' and 5'-GCTTGTCATCGTCGTCCTTGTAGTCCATCTGCA-3' . The original plasmid was pLV-CMV-IRES-eGFP [66]. We refer to the expressed protein as FLAG-SUMO-2. GFP-JARID1B and GFP-JARID1C constructs were kind gifts from Petra de Graaf and Marc Timmers (Utrecht, The Netherlands) [67].

Treatments, transfection & lentiviral infection

Cells were treated with 0.02% MMS and/or treated with 10 μM MG-132 dissolved in DMSO for the indicated amount of time. Overnight treatments with MMS were performed with a gradient dose from 0.002% to 0.005%. Arsenic trioxide (As_2O_3) was dissolved in 1M NaOH at a concentration of 280 mM, diluted to 1 mM in PBS, and used as a 1000x stock for cellular treatment with 1 μM As_2O_3 for 4 hours. For transfection, cells were cultured in DMEM lacking penicillin and streptomycin. Transfections were performed using 2.5 μg of polyethylenimine (PEI) per 1 μg of plasmid DNA, using 1 μg of DNA per 1 million cells. Transfection reagents were mixed in 150 mL NaCl and incubated for 15 minutes before adding it directly to the cells. Cells were split after 24 hours (if applicable) and investigated after 48 hours. Lentiviruses were generated essentially as described previously [68]. Infections were performed with a multiplicity of infection of 2 and using a concentration of 8 μg/mL polybrene in the medium. 24 hours after infection the medium was replaced. Cells were split 72 hours after infection (if applicable) and investigated 96 hours after infection. Lentiviral depletion of JARID1B was performed using clones TRCN0000014759 and TRCN0000014760 from the MISSION™ shRNA Library (Sigma). Lentiviral depletion of RNF4 was performed using clone TRCN0000017054 from the MISSION™ shRNA Library (Sigma). Non-targeting shRNA SHC002 from the MISSION™ shRNA Control Vectors (Sigma) was used as a control virus.

Cell culture & cell line generation

HeLa and U2OS cells were cultured in Dulbecco's Modified Eagle's Medium (DMEM) supplemented with 10% FBS and 100 U/mL penicillin and streptomycin (Invitrogen). HeLa cells stably expressing FLAG-SUMO-2 were generated through lentiviral infection with a virus encoding FLAG-SUMO-2-IRES-GFP. U2OS cells stably expressing His-SUMO-2 were generated in a similar fashion using a lentiviral construct carrying His-SUMO-2-IRES-GFP. Two weeks after infection, cells were fluorescence-sorted for a low expression level of GFP using a FACSAria II (BD Biosciences).

SILAC labeling & MMS treatment

HeLa cells were cultured in DMEM supplemented with 10% dialyzed FBS and containing either light ($[^{12}C_6{}^{14}N_2]$lysine/$[^{12}C_6{}^{14}N_4]$arginine), medium ($[^{2}H_4{}^{12}C_6{}^{14}N_2]$lysine/$[^{13}C_6{}^{14}N_4]$arginine) or heavy ($[^{13}C_6{}^{15}N_2]$lysine/$[^{13}C_6{}^{15}N_4]$arginine) lysines and arginines. Light label is referred to as K0/R0, medium label as K4/R6, and heavy label as K8/R10. Cells were cultured in SILAC DMEM for one week, during which they were passaged twice, prior to treatment and lysis. The MMS treatment experiment was carried out in duplicate with a label-swap, with the MMS-treated FLAG-SUMO-2 cell line being heavy-labeled and light-labeled in separate biological replicates, and the mock treated FLAG-SUMO-2 cell line being light-labeled and medium-labeled, respectively. The HeLa parental control was included in the second replicate using heavy-label. FLAG-SUMO-2 cells were treated with 0.02% MMS for a duration of 90 minutes.

Purification of FLAG-SUMO-2

Cells were washed three times on the plate with ice-cold PBS, prior to scraping cells and collecting them in a tube. Cells were centrifuged at 250 RCF and washed once with ice-cold PBS, and all PBS was aspirated after the final wash. Subsequently, the cell pellets were lysed vigorously on a vortex in 4 pellet volumes of Lysis Buffer (1% SDS, 0.5% NP-40, 5 mM sodium fluoride, 1 mM sodium orthovanadate, 5mM β-glycerol phosphate, 5mM sodium pyrophosphate, 0.5 mM EGTA, 5 mM 1,10-phenanthroline, all buffered in PBS, with every 10 mL of Lysis Buffer supplemented by one tablet of protease inhibitors + EDTA (Roche)). Following complete lysis, the lysates were snap frozen using liquid nitrogen, and optionally stored at -80 °C. Lysates were thawed at 30 °C and supplemented with chloroacetamide (CAA) to a final concentration of 70 mM, and immediately subjected to sonication using a microtip sonicator at a power of 30 Watts, for 20 seconds. Lysates were equalized using the bicinchoninic acid assay (BCA, Pierce), and for SILAC experiments mixed in equimolar ratio. Subsequently, lysates were diluted using one buffer volume of ice-cold Dilution Buffer (2% Triton-X100, 0.5% sodium deoxycho-

late, 1% bovine serum albumin, 5 mM sodium fluoride, 1 mM sodium orthovanadate, 5mM β-glycerol phosphate, 5mM sodium pyrophosphate, 0.5 mM EGTA, 5 mM 1,10-phenanthroline, all buffered in PBS, with every 10 mL of Dilution Buffer supplemented by one tablet of protease inhibitors + EDTA (Roche), and just before use CAA added to 70 mM). After addition of Dilution Buffer, lysates were kept on ice. Lysates were transferred to centrifuge tubes and centrifuged at 16.000 RCF for 45 minutes at 4 °C. Following centrifugation, lysates were transferred to fresh tubes while carefully avoiding disturbing the pellet. 30 µL (dry volume) FLAG-M2 agarose beads (Sigma) were prepared per 1 mL diluted lysate, by washing them four times with ice-cold Wash buffer (50 mM TRIS pH 7.5, 150 mM sodium chloride, 0.5% NP-40, 5 mM sodium fluoride, 1 mM sodium orthovanadate, 5mM β-glycerol phosphate, 5mM sodium pyrophosphate, 0.5 mM EGTA, 5 mM 1,10-phenanthroline, with every 10 mL of Wash Buffer supplemented by one tablet of protease inhibitors + EDTA (Roche)). The equilibrated beads were added to the lysates and allowed to tumble at 4 °C for 90 minutes. Following incubation, beads were pelleted by centrifugation at 500 RCF, and washed 5 times with at least 10 volumes Wash Buffer freshly supplemented with 70 mM CAA. During the second and fourth washes, the tubes were exchanged. Proteins were eluted using one buffer volume of 1 mM FLAG M2 epitope peptide in Wash Buffer, and secondly eluted using one buffer volume of 1 mM FLAG M2 epitope peptide in Wash Buffer supplemented with 5% SDS.

Purification of His-SUMO-2

Purification of His-SUMO-2-modified proteins was essentially performed as described previously [6]. HeLa or U2OS cells expressing His-SUMO-2 were washed and collected in ice-cold PBS. Cells were vigorously lysed in 25 pellet volumes of guanidine lysis buffer (6 M guanidine-HCl, 0.1 M Na2HPO4/NaH2PO4, 0.01 M TRIS, pH 8.0 and competing imidazole. Lysates were homogenized by sonication, and equalized using the BCA Protein Assay Reagent (Thermo). His-SUMO-2 conjugates were enriched using Ni-NTA beads (Qiagen) after which the beads were washed using wash buffers A to D. Wash buffer A: 6 M guanidine-HCl, 0.1 M Na2HPO4/NaH2PO4, 0.01 M TRIS, pH 8.0, 10 mM β-mercaptoethanol, 0.3% Triton X-100. Wash buffer B: 8 M urea, 0.1 M Na2HPO4/NaH2PO4, 0.01 M TRIS, pH 8.0, 10 mM β-mercaptoethanol, 0.3% Triton X-100. Wash buffer C: 8 M urea, 0.1 M Na2HPO4/NaH2PO4, 0.01 M TRIS, pH 6.3, 10 mM β-mercaptoethanol, 0.3% Triton X-100. Wash buffer D: 8 M urea, 0.1 M Na2HPO4/NaH2PO4, 0.01 M TRIS, pH 6.3, 10 mM β-mercaptoethanol, 0.1% Triton X-100. After the final wash, proteins were eluted in 7 M urea, 0.1 M Na2HPO4/NaH2PO4, 0.01 M TRIS, pH 7.0, 500 mM imidazole.

Chromatin Isolation by Biochemical Fractionation

Cellular fractionation assays were essentially performed as described previously [69].

Primary antibodies

Mouse α SUMO-2 (8A2, Abcam), Mouse α FLAG (M2, Sigma), Mouse α PML (5E10, kind gift from Prof. R van Driel, University of Amsterdam [70]), Rabbit α JARID1B (A301-813A, Bethyl), Rabbit α JARID1C (A301-035A, Bethyl), Rabbit α p300 (a kind gift from Dr. A. Zantema, Leiden University Medical Center [71]), Rabbit α CBP (A-22, Santa Cruz), Rabbit α H3K4me2 (C64G9, Cell Signaling Technology), Rabbit α PARP1 (9542L, Cell Signaling Technology), Mouse α MBD1 (IMG-306, IMGENEX), Rabbit α H3K4me3 (C42D8, Cell Signaling Technology), Rabbit α H3K9me2 (4658P, Cell Signaling Technology), Rabbit α H3K9me3 (07-442, Millipore), Rabbit α Histone H3 (06-755, Millipore), Rabbit α RNF4 (raised against GST-RNF4 [53]) and Mouse α GFP (11 814 460 001, Roche).

RNA isolation and real-time quantitative PCR

Total RNA was purified from 6 cm dishes using the SV Total RNA isolation system (Promega) according to the manufacturer's instructions. Total RNA was amplified and converted into double-stranded cDNA by reverse transcription using ImProm-II Reverse Transcriptase (Promega) and Random Hexamers (Invitrogen). Real-time quantitative PCR was performed using a CFX384 Touch Real-Time PCR detection system (Bio-Rad) in which PCR reactions were performed in a 10 µL volume containing cDNA, FastStart

Universal SYBR Green Master mix (Roche) and specific primers. The PCR was carried out with an initial denaturation at 95°C for 3 minutes, followed by 40 cycles of 95°C for 20 seconds, 55°C annealing for 20 seconds and 60°C elongation for 30 seconds. The following sense (S) and antisense (AS) primers were used: JUN (S #1) 5'-GCCAGGTCGGCAGTATAGTC-3', JUN (AS #1) 5'-GGACTCTGCCACTTGTCTCC-3', JUN (S #2) 5'-GCTGCTCTGGGAAGTGAGTT-3', JUN (AS #2) 5'-TTTCTCTAAGAGCGCACGCA-3', MCL1 (S #1) 5'-GCTCTCTCAGCCCAAAGTGA-3', MCL1 (AS #1) 5'-TGATACGGCGTCCATACCAC-3', MCL1 (S #2) 5'-AGCTCTCTCAGCCCAAAGTG-3', MCL1 (AS #2) 5'-GGCGTCCATACCACCCATTT-3', CAPNS1 (S) 5'-ATGGTTTTGGCATTGACACATG-3', CAPNS1 (AS) 5'- GCTTGCCTGTGGTGTCGC-3', ACTB (S) 5'-GACATGGAGAAAATCTGGCA-3', ACTB (AS) 5'-AATGTCACGCACGATTTCCC-3', SRPR (S) 5'-CATTGCTTTTGCACGTAACCAA-3', SRPR (AS) 5'-ATTGTCTTGCATGCGGCC-3', HMBS (S) 5'-GGCAATGCGGCTGCAA-3', HMBS (AS) 5'-GGGTACCCACGCGAATCAC-3'. Data was analyzed with the Bio-Rad CFX3 Manager software, and average RNA expression levels of triplicates were normalized for *SRPR*, *HMBS*, *CAPNS1* and *ACTB* expression levels.

Electrophoresis and immunoblotting

Protein samples were size-fractioned on Novex 4-12% Bis-Tris gradient gels using MOPS running buffer (Invitrogen), Novex 3-8% Tris-Acetate gradient gels using Tris-Acetate running buffer (Invitrogen), or on regular SDS-PAGE gels with a Tris-Glycine running buffer. Size-separated proteins were transferred to Hybond-C membranes (Amersham Biosciences) using a submarine system (Invitrogen). Membranes were stained for total protein loading using Ponceau-S (Sigma). Membranes were blocked using PBS containing 0.1% Tween-20 (PBST) and 5% milk powder for one hour. Subsequently, membranes were incubated with primary antibodies as indicated, in blocking solution. Incubation with primary antibody was performed overnight at 4 °C. Afterwards, membranes were washed three times with PBST and briefly blocked again with blocking solution. Next, membranes were incubated with secondary antibodies (donkey-anti-mouse-HRP or rabbit-anti-goat-HRP) for one hour, before washing three times with PBST and two times with PBS. Membranes were then treated with ECL2 (Pierce) as per manufacturer's instructions, and chemiluminescence was captured using Biomax XAR film (Kodak).

Electrophoresis, Coomassie Staining and In-gel digestion

Purified FLAG-SUMO-2 conjugates were size-separated by SDS-PAGE using Novex 4-12% gradient gels and MES SDS running buffer (Invitrogen), followed by staining with the Colloidal Blue Kit (Invitrogen) according to the instructions of the manufacturer. Gel lanes were excised as ten slices per eluted fraction, cut into 2 mm^3 cubes and in-gel digested with sequencing-grade modified trypsin (Promega) as described (Shevchenko et al., 2006).

LC-MS/MS analysis

The peptides extracted from the gel after digestion were cleaned, desalted and concentrated on C18 reverse phase StageTips [72], before being eluted twice with 10 µL 40% acetonitrile in 0.5% acetic acid prior to online nanoflow liquid chromatography-tandem mass spectrometry. The analysis of in-gel digested samples was initially performed using an EASY-nLC system connected to an LTQ-Orbitrap Velos (Thermo) using Higher-Collisional Dissociation (HCD) fragmentation, and the second replicate was analyzed on a Q-Exactive (Thermo) using HCD fragmentation. Separation of peptides was performed using a 15 cm analytical column packed in-house with 3 µm C18 beads (Reprosil, Dr Maisch), using a 80 minute gradient from 8% to 75% acetonitrile in 0.5% acetic acid, and a flow rate of 250 nL/minute. The mass spectrometers were operated in data-dependent acquisition mode using a top 10 method. LTQ-Orbitrap Velos full-scan MS spectra were acquired with a target value of 1E6 and a resolution of 30,000, and the HCD tandem MS/MS spectra were acquired using a target value of 5E4, a resolution of 7,500, and a normalized collision energy of 35%. Q-Exactive full-scan MS spectra were acquired with a target value of 1E6 and a resolution of 70,000, and the HCD tandem MS/MS spectra were acquired using a target value of 1E6, a resolution of 35,000, and a normalized collision energy of 25%.

Data processing and analysis

MaxQuant version 1.2.2.9 was used to analyze the RAW data [73, 74]. Precursor MS signal intensities were determined and SILAC duplets or triplets were automatically quantified. MS/MS spectra were filtered and deisotoped, and only the 10 most abundant fragments for each 100 mass/charge (m/z) range were retained. Protein identification was performed by matching the identified MS/MS spectra versus a target/decoy version of the complete human Uniprot database, supplemented by a database of commonly observed mass spectrometry contaminants. MS/MS spectra were accepted with a mass tolerance of 4.5 ppm on precursor masses, and a tolerance of 20 ppm for fragment ions. Cysteine carbamidomethylation was searched as a fixed modification, and protein N-terminal acetylation and methionine oxidation were searched as variable modifications. The processed data was individually filtered for each experimental replicate by posterior error probability (PEP) to achieve a protein false discovery rate (FDR) of below 1%.

Data from two separate label-swapped experiments was combined and filtered using Perseus [75]. SUMO/Parental ratio was calculated by averaging the 2-log ratios of both MMS-treated and mock-treated FLAG-SUMO2 cells compared to parental cells, and SUMO-modified targets were filtered with a 2-log SUMO/Parental ratio requirement of greater than 0.5 in either the control treatment or MMS treatment, with an additional requirement of a ratio greater than 0.25 when control and MMS enrichments were averaged. MMS/Control ratio normalization was performed around the 2-log MMS/Control ratio of SUMO-2. SUMO-regulated targets were identified with a 2-log MMS/Control ratio requirement of less than -0.5 or greater than 0.5 averaged over the duplicate, and a 2-log MMS/Control ratio requirement of less than -0.25 or greater than 0.25 individually in both experiments. Regardless of MMS/Control ratio, only proteins that passed the SUMO/Parental check were used in subsequent analyses. Gene Ontology (GO) analysis was performed using Perseus to compare SUMO upregulated or SUMO downregulated targets versus the GOBP, GOCC, GOMF, keywords, GSEA and Pfam annotated human proteome, using Fisher Exact testing. Benjamini and Hochberg FDR was applied to p-values to correct for multiple hypotheses testing, and final corrected p-values were filtered to be less than 0.05. STRING network analysis was performed using the online STRING database [76], using all SUMO regulated targets as input, and allowing interactions with medium or greater confidence ($p>0.4$).

Microscopy

Cells were seeded on glass coverslips, and fixed 24 hours later for 10 minutes in 3.7% paraformaldehyde in PHEM buffer (60 mM PIPES, 25 mM HEPES, 10 mM EGTA, 2 mM $MgCl_2$ pH 6.9) at 37 °C. After washing with PBS, cells were permeabilized with 0.1% Triton-X100 for 10 minutes, washed with PBST, and blocked using TNB (100 mM TRIS pH 7.5, 150 mM NaCl, 0.5% Blocking Reagent (Roche)) for 30 minutes. Cells were incubated with primary antibody as indicated, in TNB for one hour. Subsequently cells were washed five times with PBST, and incubated with secondary antibodies (Goat α Mouse Alexa 488 and Goat α Rabbit Alexa 594 (Invitrogen)) in TNB for one hour. Next, cells were washed five times with PBST and dehydrated using alcohol, prior to embedding them in Citifluor (Agar Scientific) containing 400 ng/µL DAPI (Sigma) and sealing the slides with nail varnish. Images were recorded on a Leica SP5 confocal microscope system using 488 nm and 561 nm lasers for excitation, a 63X lens for magnification, and were analyzed with Leica confocal software. For quantification of PML bodies, groups of cells were recorded in similar-sized fields using Z-stacking with steps of 0.5 µm to acquire 10 images ranging from the bottom to the top of the cells. Images were maximum projected, individual cells were localized and PML bodies were counted using in-house image analysis software Stacks [77].

ACKNOWLEDGMENTS

This work was supported by the Netherlands Organization for Scientific Research (NWO) (A.C.O.V.), ZonMW (A.C.O.V.), the European Research Council (A.C.O.V) and the research career program FSS Sapere Aude (J.V.O.) from the Danish Research

Council. The NNF Center for Protein Research is supported by a generous donation from the Novo Nordisk Foundation. We want to thank Rene Overmeer and Sander Tuit for assistance during the early phase of this project. We are grateful to Drs. H.T. Timmers, P. de Graaf, R. van Driel and A. Zantema for providing critical reagents.

Reference List

1. Vertegaal, A. C. (2011) Uncovering ubiquitin and ubiquitin-like signaling networks. *Chem. Rev.* 111, 7923-7940
2. Flotho, A., and Melchior, F. (2013) Sumoylation: a regulatory protein modification in health and disease. *Annu. Rev. Biochem.* 82, 357-385
3. Ulrich, H. D., and Walden, H. (2010) Ubiquitin signalling in DNA replication and repair. *Nat. Rev. Mol. Cell Biol.* 11, 479-489
4. Hickey, C. M., Wilson, N. R., and Hochstrasser, M. (2012) Function and regulation of SUMO proteases. *Nat. Rev. Mol. Cell Biol.* 13, 755-766
5. Golebiowski, F. et al. (2009) System-wide changes to SUMO modifications in response to heat shock. *Sci. Signal.* 2, ra24
6. Matic, I. et al. (2010) Site-specific identification of SUMO-2 targets in cells reveals an inverted SUMOylation motif and a hydrophobic cluster SUMOylation motif. *Mol. Cell* 39, 641-652
7. Jackson, S. P., and Durocher, D. (2013) Regulation of DNA damage responses by ubiquitin and SUMO. *Mol. Cell* 49, 795-807
8. Stelter, P., and Ulrich, H. D. (2003) Control of spontaneous and damage-induced mutagenesis by SUMO and ubiquitin conjugation. *Nature* 425, 188-191
9. Hoege, C., Pfander, B., Moldovan, G. L., Pyrowolakis, G., and Jentsch, S. (2002) RAD6-dependent DNA repair is linked to modification of PCNA by ubiquitin and SUMO. *Nature* 419, 135-141
10. Galanty, Y. et al. (2009) Mammalian SUMO E3-ligases PIAS1 and PIAS4 promote responses to DNA double-strand breaks. *Nature* 462, 935-939
11. Morris, J. R. et al. (2009) The SUMO modification pathway is involved in the BRCA1 response to genotoxic stress. *Nature* 462, 886-890
12. Silver, H. R., Nissley, J. A., Reed, S. H., Hou, Y. M., and Johnson, E. S. (2011) A role for SUMO in nucleotide excision repair. *DNA Repair (Amst)* 10, 1243-1251
13. Geiss-Friedlander, R., and Melchior, F. (2007) Concepts in sumoylation: a decade on. *Nat. Rev. Mol. Cell Biol.* 8, 947-956
14. Silva, A., Vitorino, R., Domingues, M. R., Spickett, C. M., and Domingues, P. (2013) Post-translational Modifications and Mass Spectrometry Detection. *Free Radic. Biol. Med.*
15. Choudhary, C., and Mann, M. (2010) Decoding signalling networks by mass spectrometry-based proteomics. *Nat. Rev. Mol. Cell Biol.* 11, 427-439
16. Yang, W. et al. (2012) Analysis of oxygen/glucose-deprivation-induced changes in SUMO3 conjugation using SILAC-based quantitative proteomics. *J. Proteome. Res.* 11, 1108-1117
17. Wang, Y., and Dasso, M. (2009) SUMOylation and deSUMOylation at a glance. *J. Cell Sci.* 122, 4249-4252
18. Saitoh, H., and Hinchey, J. (2000) Functional heterogeneity of small ubiquitin-related protein modifiers SUMO-1 versus SUMO-2/3. *J. Biol. Chem.* 275, 6252-6258

19. Maeda, D. et al. (2004) Ubc9 is required for damage-tolerance and damage-induced interchromosomal homologous recombination in S. cerevisiae. *DNA Repair (Amst)* 3, 335-341
20. Psakhye, I., and Jentsch, S. (2012) Protein group modification and synergy in the SUMO pathway as exemplified in DNA repair. *Cell* 151, 807-820
21. Johnson, E. S. (2004) Protein modification by SUMO. *Annu. Rev. Biochem.* 73, 355-382
22. Girdwood, D. et al. (2003) P300 transcriptional repression is mediated by SUMO modification. *Mol. Cell* 11, 1043-1054
23. Muller, S., and Dejean, A. (1999) Viral immediate-early proteins abrogate the modification by SUMO-1 of PML and Sp100 proteins, correlating with nuclear body disruption. *J. Virol.* 73, 5137-5143
24. Ishov, A. M. et al. (1999) PML is critical for ND10 formation and recruits the PML-interacting protein daxx to this nuclear structure when modified by SUMO-1. *J. Cell Biol.* 147, 221-234
25. Shen, T. H., Lin, H. K., Scaglioni, P. P., Yung, T. M., and Pandolfi, P. P. (2006) The mechanisms of PML-nuclear body formation. *Mol. Cell* 24, 331-339
26. Sun, H., Leverson, J. D., and Hunter, T. (2007) Conserved function of RNF4 family proteins in eukaryotes: targeting a ubiquitin ligase to SUMOylated proteins. *EMBO J.* 26, 4102-4112
27. Tatham, M. H. et al. (2008) RNF4 is a poly-SUMO-specific E3 ubiquitin ligase required for arsenic-induced PML degradation. *Nat. Cell Biol.* 10, 538-546
28. Brouwer, A. K. et al. (2009) Telomeric DNA mediates de novo PML body formation. *Mol. Biol. Cell* 20, 4804-4815
29. Bernardi, R., and Pandolfi, P. P. (2007) Structure, dynamics and functions of promyelocytic leukaemia nuclear bodies. *Nat. Rev. Mol. Cell Biol.* 8, 1006-1016
30. Svejstrup, J. Q. (2010) The interface between transcription and mechanisms maintaining genome integrity. *Trends Biochem. Sci.* 35, 333-338
31. Fry, R. C., Begley, T. J., and Samson, L. D. (2005) Genome-wide responses to DNA-damaging agents. *Annu. Rev. Microbiol.* 59, 357-377
32. Begley, T. J., and Samson, L. D. (2004) Network responses to DNA damaging agents. *DNA Repair (Amst)* 3, 1123-1132
33. Jelinsky, S. A., and Samson, L. D. (1999) Global response of Saccharomyces cerevisiae to an alkylating agent. *Proc. Natl. Acad. Sci. U. S. A* 96, 1486-1491
34. Chi, P., Allis, C. D., and Wang, G. G. (2010) Covalent histone modifications--miswritten, misinterpreted and mis-erased in human cancers. *Nat. Rev. Cancer* 10, 457-469
35. Neyret-Kahn, H. et al. (2013) Sumoylation at chromatin governs coordinated repression of a transcriptional program essential for cell growth and proliferation. *Genome Res.*
36. Lyst, M. J., Nan, X., and Stancheva, I. (2006) Regulation of MBD1-mediated transcriptional repression by SUMO and PIAS proteins. *EMBO J.* 25, 5317-5328
37. Ouyang, J., and Gill, G. (2009) SUMO engages multiple corepressors to regulate chromatin structure and transcription. *Epigenetics.* 4, 440-444
38. Sterner, D. E., and Berger, S. L. (2000) Acetylation of histones and transcription-related factors. *Microbiol. Mol. Biol. Rev.* 64, 435-459
39. Bueno, M. T., and Richard, S. (2013) SUMOylation negatively modulates target gene occupancy of the KDM5B, a histone lysine demethylase. *Epigenetics.* 8
40. Xiang, Y. et al. (2007) JARID1B is a histone

H3 lysine 4 demethylase up-regulated in prostate cancer. *Proc. Natl. Acad. Sci. U. S. A* 104, 19226-19231

41. Roesch, A. et al. (2008) RBP2-H1/JARID1B is a transcriptional regulator with a tumor suppressive potential in melanoma cells. *Int. J. Cancer* 122, 1047-1057
42. Mitra, D., Das, P. M., Huynh, F. C., and Jones, F. E. (2011) Jumonji/ARID1 B (JARID1B) protein promotes breast tumor cell cycle progression through epigenetic repression of microRNA let-7e. *J. Biol. Chem.* 286, 40531-40535
43. Kandoth, C. et al. (2013) Mutational landscape and significance across 12 major cancer types. *Nature* 502, 333-339
44. Messner, S. et al. (2009) Sumoylation of poly(ADP-ribose) polymerase 1 inhibits its acetylation and restrains transcriptional coactivator function. *FASEB J.* 23, 3978-3989
45. Messner, S. et al. (2010) PARP1 ADP-ribosylates lysine residues of the core histone tails. *Nucleic Acids Res.* 38, 6350-6362
46. Krishnakumar, R., and Kraus, W. L. (2010) PARP-1 regulates chromatin structure and transcription through a KDM5B-dependent pathway. *Mol. Cell* 39, 736-749
47. Rasheed, Z. A., Saleem, A., Ravee, Y., Pandolfi, P. P., and Rubin, E. H. (2002) The topoisomerase I-binding RING protein, topors, is associated with promyelocytic leukemia nuclear bodies. *Exp. Cell Res.* 277, 152-160
48. Pungaliya, P. et al. (2007) TOPORS functions as a SUMO-1 E3 ligase for chromatin-modifying proteins. *J. Proteome. Res.* 6, 3918-3923
49. Moilanen, A. M. et al. (1998) Identification of a novel RING finger protein as a coregulator in steroid receptor-mediated gene transcription. *Mol. Cell Biol.* 18, 5128-5139
50. Poukka, H., Aarnisalo, P., Santti, H., Janne, O. A., and Palvimo, J. J. (2000) Coregulator small nuclear RING finger protein (SNURF) enhances Sp1- and steroid receptor-mediated transcription by different mechanisms. *J. Biol. Chem.* 275, 571-579
51. Kosoy, A., Calonge, T. M., Outwin, E. A., and O'Connell, M. J. (2007) Fission yeast Rnf4 homologs are required for DNA repair. *J. Biol. Chem.* 282, 20388-20394
52. Guzzo, C. M. et al. (2012) RNF4-dependent hybrid SUMO-ubiquitin chains are signals for RAP80 and thereby mediate the recruitment of BRCA1 to sites of DNA damage. *Sci. Signal.* 5, ra88
53. Vyas, R. et al. (2013) RNF4 is required for DNA double-strand break repair in vivo. *Cell Death Differ.* 20, 490-502
54. Yin, Y. et al. (2012) SUMO-targeted ubiquitin E3 ligase RNF4 is required for the response of human cells to DNA damage. *Genes Dev.* 26, 1196-1208
55. Galanty, Y., Belotserkovskaya, R., Coates, J., and Jackson, S. P. (2012) RNF4, a SUMO-targeted ubiquitin E3 ligase, promotes DNA double-strand break repair. *Genes Dev.* 26, 1179-1195
56. Luo, K., Zhang, H., Wang, L., Yuan, J., and Lou, Z. (2012) Sumoylation of MDC1 is important for proper DNA damage response. *EMBO J.* 31, 3008-3019
57. Lallemand-Breitenbach, V. et al. (2008) Arsenic degrades PML or PML-RARalpha through a SUMO-triggered RNF4/ubiquitin-mediated pathway. *Nat. Cell Biol.* 10, 547-555
58. Poulsen, S. L. et al. (2013) RNF111/Arkadia is a SUMO-targeted ubiquitin ligase that facilitates the DNA damage response. *J. Cell Biol.* 201, 797-807
59. Lin, D. Y. et al. (2006) Role of SUMO-interacting motif in Daxx SUMO modification, subnuclear localization, and repression of

sumoylated transcription factors. *Mol. Cell* 24, 341-354

60. Boichuk, S., Hu, L., Makielski, K., Pandolfi, P. P., and Gjoerup, O. V. (2011) Functional connection between Rad51 and PML in homology-directed repair. *PLoS. One.* 6, e25814
61. Dellaire, G., and Bazett-Jones, D. P. (2004) PML nuclear bodies: dynamic sensors of DNA damage and cellular stress. *Bioessays* 26, 963-977
62. Lachner, M., O'Carroll, D., Rea, S., Mechtler, K., and Jenuwein, T. (2001) Methylation of histone H3 lysine 9 creates a binding site for HP1 proteins. *Nature* 410, 116-120
63. Bannister, A. J. et al. (2001) Selective recognition of methylated lysine 9 on histone H3 by the HP1 chromo domain. *Nature* 410, 120-124
64. Sternsdorf, T., Jensen, K., Reich, B., and Will, H. (1999) The nuclear dot protein sp100, characterization of domains necessary for dimerization, subcellular localization, and modification by small ubiquitin-like modifiers. *J. Biol. Chem.* 274, 12555-12566
65. Tatham, M. H. et al. (2001) Polymeric chains of SUMO-2 and SUMO-3 are conjugated to protein substrates by SAE1/SAE2 and Ubc9. *J. Biol. Chem.* 276, 35368-35374
66. Vellinga, J. et al. (2006) A system for efficient generation of adenovirus protein IX-producing helper cell lines. *J. Gene Med.* 8, 147-154
67. Outchkourov, N. S. et al. (2013) Balancing of histone H3K4 methylation states by the Kdm5c/SMCX histone demethylase modulates promoter and enhancer function. *Cell Rep.* 3, 1071-1079
68. Tiscornia, G., Singer, O., and Verma, I. M. (2006) Production and purification of lentiviral vectors. *Nat. Protoc.* 1, 241-245
69. Wysocka, J., Reilly, P. T., and Herr, W. (2001) Loss of HCF-1-chromatin association precedes temperature-induced growth arrest of tsBN67 cells. *Mol. Cell Biol.* 21, 3820-3829
70. Stuurman, N. et al. (1992) A monoclonal antibody recognizing nuclear matrix-associated nuclear bodies. *J. Cell Sci.* 101 (Pt 4), 773-784
71. Ramos, Y. F. et al. (2010) Genome-wide assessment of differential roles for p300 and CBP in transcription regulation. *Nucleic Acids Res.* 38, 5396-5408
72. Rappsilber, J., Mann, M., and Ishihama, Y. (2007) Protocol for micro-purification, enrichment, pre-fractionation and storage of peptides for proteomics using StageTips. *Nat. Protoc.* 2, 1896-1906
73. Cox, J. et al. (2011) Andromeda: a peptide search engine integrated into the MaxQuant environment. *J. Proteome. Res.* 10, 1794-1805
74. Cox, J., and Mann, M. (2008) MaxQuant enables high peptide identification rates, individualized p.p.b.-range mass accuracies and proteome-wide protein quantification. *Nat. Biotechnol.* 26, 1367-1372
75. Cox, J., and Mann, M. (2012) 1D and 2D annotation enrichment: a statistical method integrating quantitative proteomics with complementary high-throughput data. *BMC. Bioinformatics.* 13 Suppl 16, S12
76. Franceschini, A. et al. (2013) STRING v9.1: protein-protein interaction networks, with increased coverage and integration. *Nucleic Acids Res.* 41, D808-D815
77. Smeenk, G. et al. (2010) The NuRD chromatin-remodeling complex regulates signaling and repair of DNA damage. *J. Cell Biol.* 190, 741-749

A STRING Network Analysis of SUMO-regulated proteins in response to MMS
Expanded by 10% highest predicted network interactors -- 47% clustered (40/85)

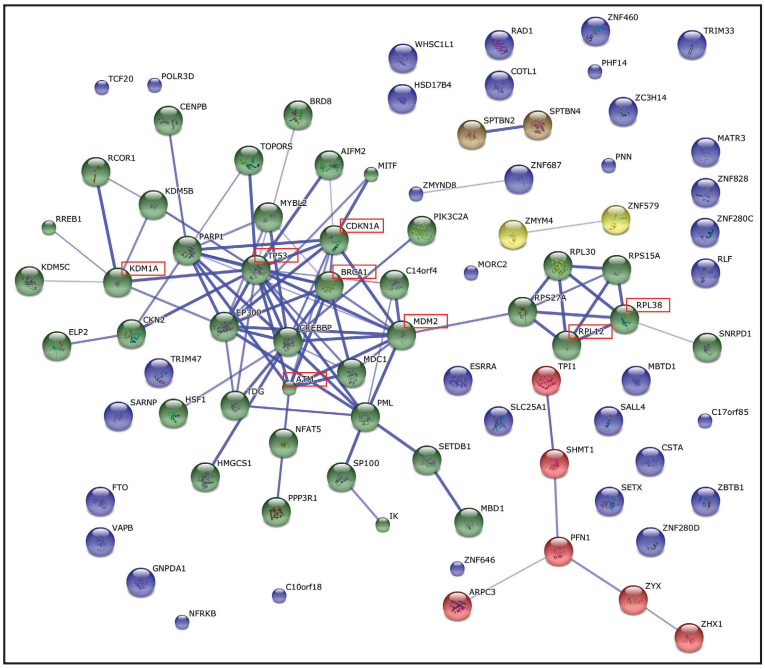

B STRING Network Analysis of SUMO-regulated proteins in response to MMS
Expanded by insertion of SUMO2 -- 68% clustered (53/78)

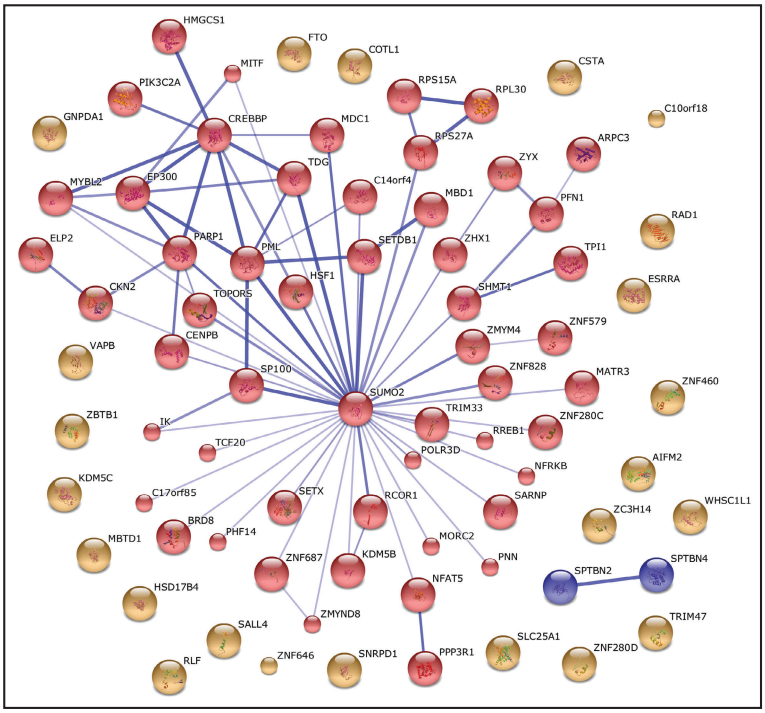

Figure S1. Expansion of the main interaction clusters by highest predicted interactors or SUMO provides evidence towards protein group modification in response to MMS.
A) STRING network analysis of all regulated SUMOylated proteins in response to MMS, expanded by 10% (8) highest predicted interactor nodes. Additional nodes are boxed in red. Network expansion placed 40 out of 85 proteins (47%) in one single interaction network, with 52 out of 85 proteins (61%) being part of any network.
B) STRING network analysis of all regulated SUMOylated proteins in response to MMS, expanded by addition of *SUMO2* as a node. Network expansion placed 53 out of 78 proteins (68%) in one single interaction network.

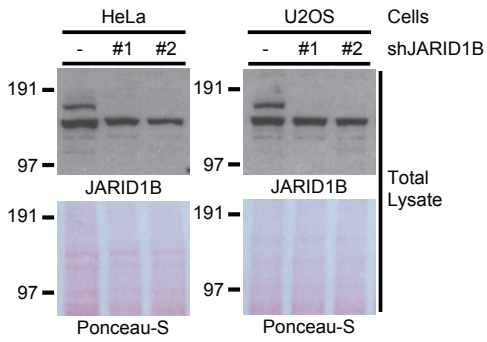

Figure S2. Knockdown of JARID1B confirms the upper immunoblot band as corresponding to endogenous JARID1B in total lysates.
HeLa cells and U2OS cells were depleted of endogenous JARID1B by infection with lentiviruses encoding two different shRNAs against JARID1B, or were treated with an untargeted lentivirus. Cells were lysed, and total lysates were analyzed by immunoblotting to confirm which band corresponds to endogenous JARID1B. Ponceau-S staining was performed on the total lysates as a loading control.

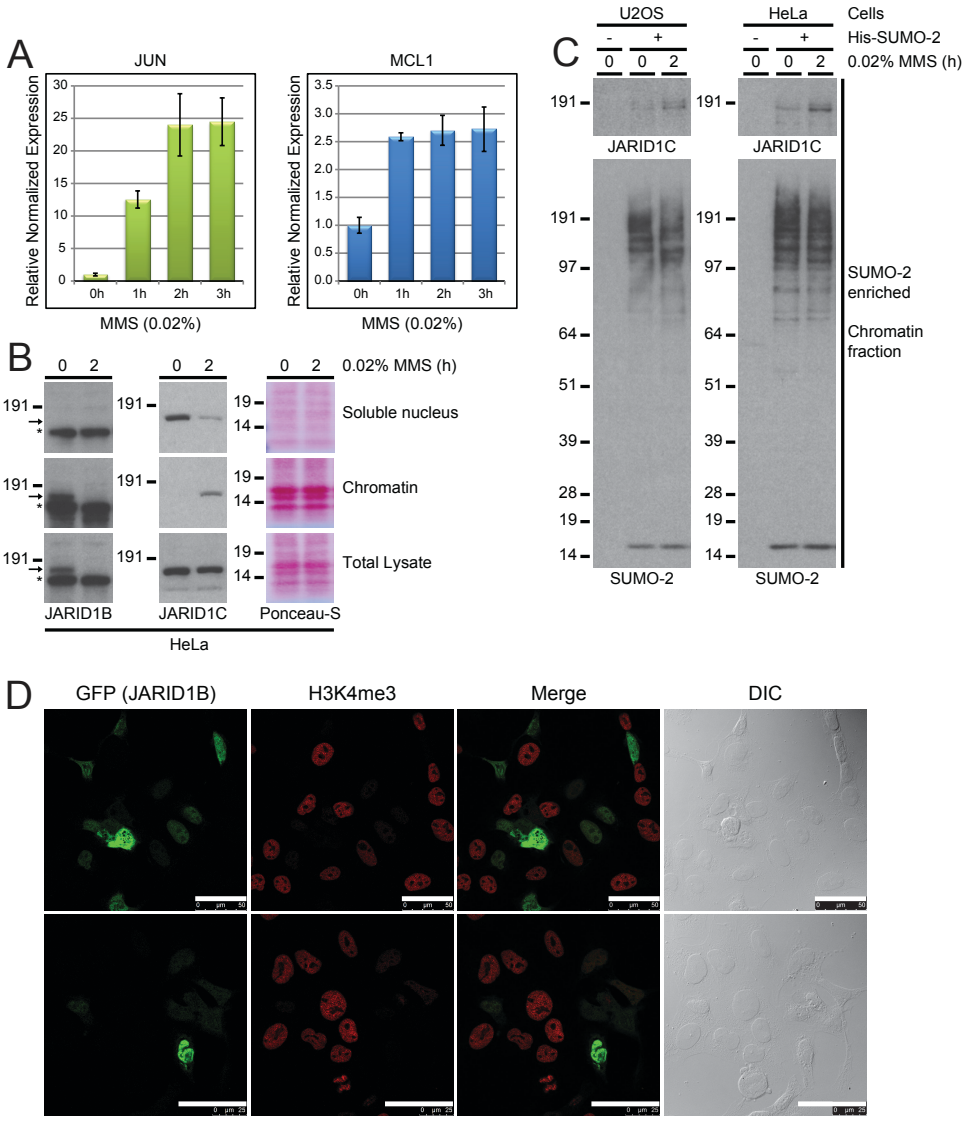

Figure S3. Known JARID1B targets *JUN* and *MCL1* are transcriptionally upregulated in response to MMS treatment. JARID1C is recruited to the chromatin upon MMS treatment in HeLa cells, and SUMOylated JARID1C is detectable at the chromatin.

A) U2OS cells were mock treated or treated with 0.02% MMS for the indicated amounts of time, and subsequently the cells were lysed and RNA was isolated. Quantitative PCR was performed using two distinct sets of primers versus both *JUN* and *MCL1*. The average expression levels of triplicates were normalized versus the housekeeping genes *SRPR*, *HMBS*, *CAPNS1* and *ACTB*. RNA expression shown is relative to untreated U2OS. Error bars represent standard deviation. All differences between untreated and MMS treated values are significant with $p < 0.03$.

B) HeLa cells were mock treated or treated with 0.02% MMS for 90 minutes, and subsequently cellular fractionation was performed to separate the soluble nucleoplasmic fraction from the chromatin. Soluble nucleoplasmic fractions, chromatin fractions, and total lysates were analyzed

by immunoblotting for JARID1B and JARID1C. Ponceau-S staining of the histones is shown as a loading and fractionation control.
C) U2OS cells and HeLa cells stably expressing His-tagged SUMO-2, as well as the corresponding parental cell lines, were treated as in Figure S3A. After isolation of the chromatin fraction, His-pull-down was performed to enrich SUMOylated proteins located at the chromatin. SUMO-enriched chromatin fractions were analyzed by immunoblotting for JARID1C. Immunoblotting for SUMO-2 was performed as a pulldown and loading control.
D) U2OS cells were transfected with GFP-JARID1B. Subsequently, cells were fixed and investigated by confocal fluorescent microscopy to check for the presence of JARID1B (GFP) and the level of H3K4me3. The presence of GFP-JARID1B resulted in an intense drop of global H3K4me3, even at relatively low expression levels. Scale bars represent 50 µm.